# Real-Time TRMM Multi-Satellite Precipitation Analysis Data Set Documentation

George J. Huffman (1) David T. Bolvin (1,2)

(1) Mesoscale Atmospheric Processes Laboratory, NASA Goddard Space Flight Center (2) Science Systems and Applications, Inc.

26 April 2018

#### **News About the TMPA-RT**

26 April 2018 DOIs have been assigned for 3B40RT, 3B41RT, and 3B42RT.

10 May 2016 The data flow from the Himawari-8 GEO satellite was interrupted for 57 hours, 7 May, 05 UTC – 9 May, 14 UTC and during that time there are patches of missing values in the 3B42RT data, and continuous zones of missing values in the 3B41RT data in the center of the Himawari-8 sector (over Japan), where data from the adjoining satellites are unable to fill the gap.

14 January 2016 A system configuration problem caused failures in the microwave precipitation gridding, leading to 3B42RT only containing IR precip estimates for a number of times. The problem was corrected and the following products were re-run:

3B40RT and 3B42RT: 13 January, UTC hours 15, 18, 21; 14 January, UTC hours 00, 03, 06, 09

3B41RT: 13 January, UTC hours 15-23; 14 January, UTC hours 00-10

4 January 2016 With the turnover of the year to 2016, the suite of 3B40RT, 3B41RT, and 3B42RT failed to process. This was traced to a very old quality control on the date/time, fixed, and retrospectively processed to give a complete time series. The affected date/times are 160101 00 UTC on 1 January 20 through 12 UTC on 2 January 2016.

20 October 2015 Corrected the statement in "data file layout" under 3B42RT to read "The leading precipitation field has a climatological bias correction to the 3B42 Version 7 estimates (see step 2 in "HQ+VAR", 3B42RT)".

7 July 2015 MTSat-2 was replaced by Himawari 8 effective 02 UTC on 7 July 2015.

28 April 2015 NOAA reprocessed the global IR data for 10 UTC 26 April through 14 UTC 27 April due to dropped images, and all 3B41RT and 3B42RT files for this time period were reprocessed by PPS:

3B41RT.2015042610.7.bin.gz through 3B41RT.2015042714.7.bin.gz 3B42RT.2015042612.7.bin.gz through 3B42RT.2015042715.7.bin.gz

17 April 2015 IR fill-ins ceased when CPC Global 4 km Merged IR data dropped out starting 16 UTC 14 April due to processing issues at NOAA, and gradually returned through 11 UTC 17 April. The 3B41RT and 3B42RT files for that time period were batch-processed:

```
3B41RT.2015041416.7.bin.gz - 3B41RT.2015041710.7.bin.gz
3B42RT.2015041418.7.bin.gz - 3B42RT.2015041709.7.bin.gz
```

8 April 2015 TMI data are no longer input to the products because they were terminated on 8 April 2015 as part of the TRMM satellite end-of-mission activities.

28 October 2014 Starting about 22 UTC on 20 October 2014, PPS discovered missing input data files originating at NOAA. This networking issue prevented the reception of sounder data, and the IR fields only contained GOES-E and -W. MHS data started flowing around 02 UTC on 23 October 2014, with full geo-IR returning around 16 UTC 23 October 2014. Specifically, 3B42RT missed both MHS and Eastern Hemisphere IR for 00 UTC 21 October through 00 UTC 23 October, and then missed Eastern Hemisphere IR through 15 UTC 23 October. Subsequently, PPS reprocessed 3B41RT and 3B42RT after NOAA forwarded revised, fully populated IR datasets. The reprocessed files produced on 28 October are:

```
3B41RT.2014102022.7.bin.gz – 3B41RT.2014102306.7.bin.gz
3B42RT.2014102021.7.bin.gz – 3B42RT.2014102306.7.bin.gz
```

However, it is not practical to recover the missing sounder data in the RT system, so the microwave content is about half the usual amount in 3B40RT and 3B42RT for the outage period: 00 UTC 21 October through 00 UTC 23 October.

- 25 May 2014 Metop-A was restored to functionality; after verification, the date were again included in the TMPA-RT starting 03 UTC on 25 May 2014.
- 28 March 2014 Metop-A had an apparent hardware failure at 14 UTC on 27 March 2014 and the instrument is off.
- 15 February 2014 Snow accumulation on the receiving antenna prevented reception of MTSAT-2 data from 1832 UTC on 14 February 2014 to 1232 UTC on 15 February 2014. The data are lost.
- 12 November 2013 A TRMM spacecraft anomaly resulted in the loss of most TRMM sensor data for the period 02-14 UTC on 12 November 2013, and additional issues resulted in data gaps during the period 20-23:30 UTC. This reduces the data content in 3B40RT and 3B42RT somewhat, but is not a serious issue overall.
- 16 August 2013 Metop-B was added as an input data source on 15 August 2013; the first time in 3B40RT was 09 UTC, and for 3B41RT (in the calibration) and 3B42RT the first time was 15 UTC.
- 28 January 2013 Processing issues were discovered with both the Version 7 TMPA production (3B42/43) and Version 7 TMPA-RT (3B40/41/42RT) data series and it was decided to re-do the retrospective processings to correct the issues. In general the original Version 7 data sets are considered an improvement over Version 6, but this additional processing is considered important to meet the goals of the project. Users are urged to switch to the newest Version 7 data sets as soon as practical. See "additional processing for Version 7" for more details.

- 13 October 2012 Due to internal processing errors, some radiometer data were not included in data files for 08 UTC 12 October 2012 through 03 UTC 13 October 2012. PPS has rerun all the affected TMPA 3B40RT, 3B41RT, and 3B42RT. The original files are probably adequate for most purposes, but the rerun data should be more accurate.
- 11 October 2012 the NOAA server providing access to sounder data went out of service from 15:51 UTC 10 October to 02 UTC 11 October. Data continued to be recorded, so at the first opportunity after the NOAA server came up, PPS retrieved the backlogged products. All the TMPA-RT products were re-run for 18 UTC 10 October through 03 UTC 11 October.
- 25 September 2012 GOES-E (GOES-13) developed problems with the sounder and some IR channels late last week. Eventually it was placed in safe mode and subsequently GOES-15 was programmed to take over GOES-E observational schedule. The TMPA-RT products affected are 3B41RT and 3B42RT, in the GOES-E sector, roughly the Americas. Recovery efforts for GOES-13 are on-going.

Visual inspection of the 3B41RT data shows some missing data during the period 23 September 22 UTC through 24 September 10 UTC. Even when the data in the GOES-E sector aren't missing, the alternative satellites used to provide the fill-in by NOAA/CPC don't necessarily exhibit the same bias characteristics from satellite to satellite, probably due to the use of data at a variety of zenith angles. Visual evidence of bias differences due to fill-in data starts at the same time, 23 September 22 UTC, and extends through 24 September 17 UTC.

- 14 September 2012 A network outage at NOAA prevented the original IR input data files from capturing all available data yesterday afternoon. This morning the IR files were re-staged for 12-16 UTC on 13 September 2012, which necessitated PPS re-running 3B41RT for 12-16 UTC and 3B42RT for 12, 15 and 18 UTC on 13 September 2012. Users should re-pull these hours of data to have the best record of TMPA-RT data.
- 25 June 2012 The new Version 7 of the TMPA-RT (not to be confused with the on-going Version 7 of the official TRMM products) was released effective 10 UTC, Monday, 25 June 2012. This is the upgrade that many of you have heard discussed for over a year, during which time we waited for the Version 7 TRMM products, the TMPA in particular, and developed an interim solution for SSMIS calibration. The new version includes the following:
- 1. SSMIS data are introduced based on interim calibration developed in conjunction with D. Vila (ESSIC).
- 2. It is planned to retrospectively process the RT system back to 1 March 2000 during July 2012 to satisfy numerous user requests for a long archive of RT data to enable calibration of real-time applications that cannot take advantage of the Version 7 TMPA archive. In this innovative approach the RT code was run on the production computer system, since the RT computer system is not equipped to do such processing. As a result, Version 7 RT data sets will be made available starting 1 March 2000. The main difference from true RT processing is that the full input satellite data sets available in the Version 7 production system are used. These production data archives are somewhat more complete than what would have been received in real time. The start date is driven by the start date of the CPC Merged 4 Km IR

- data record and the need to spin up the microwave-IR calibration. It continues to be the case that, despite the long RT record, it is strongly recommended that the production dataset (3B42) be used or all research not specifically focused on RT applications.
- 3. Upon this release RT data that pre-date Version 6 continue to be provided in subdirectory *V5*, while Version 6 RT data are moved to subdirectory *V6*.

#### **Contents**

- 1. Data Set Names and General Content
- 2. Related Projects, Data Networks, and Data Sets
- 3. Storage and Distribution Media
- 4. Reading the Data
- 5. Definitions and Defining Algorithms
- 6. Temporal and Spatial Coverage and Resolution
- 7. Production and Updates
- 8. Sensors
- 9. Error Detection and Correction
- 10. Missing Value Estimation and Codes
- 11. Quality and Confidence Estimates
- 12. Data Archives
- 13. Documentation
- 14. Inventories
- 15. How to Order and Obtain Information about the Data
- 16. Appendices
  - 16.1 Read a File of Data, C Example
  - 16.2 Read the Header Record, FORTRAN Example
  - 16.3 Read a File of Data in a Single Read, FORTRAN Example
  - 16.4 Read a File of Data, IDL Example
  - 16.5 Read a File of Data Line-at-a-Time, FORTRAN Example
  - 16.6 Read a File of Data, R Code

## **Keywords** (searchable as \*keyword\*)

2A12RT	AMSU-B
2B31	AMSU-B precipitation data set
3B40RT	AMSU-B error detection/correction
3B41RT	archive and distribution sites
3B42	controlling factors on dataset performance
3B42RT	data access policy
accuracy	data file access technique
acronyms	data file identifier
additional processing for Version 7	data file layout
ambiguous pixels	data providers
AMSR-E	data set archive
AMSR-E error detection/correction	data set creators

data set inventory precipitation variable production and updates data set name decode high-latitude VAR and HQ+VAR read a file of data precipitation values Read a File of Data, C Example decode highly ambiguous HQ precipitation Read a File of Data, IDL Example Read a File of Data In a Single Read. values diurnal cycle FORTRAN Example documentation creator Read a File of Data Line-at-a-Time, documentation revision history FORTRAN Example DOIsfor 3B40RT, 3B41RT, and 3B42RT Read a File of Data, R Code estimate missing values read the header record file date Read the Header Record, FORTRAN Giovanni Example **GPROF** references retrospective processing grid HQ sensors contributing to TMPA-RT HQ+VAR similar data sets **IMERG** spatial coverage spatial resolution interannual differences driven by data set calibrators (see "controlling factors on **SSMI** dataset performance") SSMI error detection/correction intercomparison results SSMI Level 2 precipitation estimates IR **SSMIS** IR data correction SSMIS Level 1b Ta data standard missing value known anomalies known data set access issues temporal resolution time zone known errors Merged 4-Km IR Tb data set **TMI** MHS TMI error detection/correction transition from Version 6 to Version 7 MHS precipitation data set MHS error detection/correction **TRMM** missing hours TRMM end of mission issues obtaining data units of the TMPA-RT estimates originating machine VAR period of record

#### 1. Data Set Names and General Content

The formal \*data set name\* is the "Version 7 TRMM Real-Time Multi-Satellite Precipitation Analysis." For convenience, it is referred to in this document as the "TMPA-RT." Note that there are other products in the general TRMM real-time system. Also, note that the TMPA-RT version numbering is <u>not</u> related to the official TRMM product version numbering, although both happen to be numbered 7 at the present.

precipitation phase

The data set currently contains three products, providing merged microwave, microwave-calibrated infrared (IR), and combined microwave-IR estimates of precipitation on quasi-global grids computed in near-real time starting 06 UTC 7 November 2012. Current-version retrospectively processed data are available beginning with 00 UTC 1 March 2000.

Huffman et al. (2007) is the primary refereed citation for the TMPA, Huffman et al. (2010) describe the 2009 updates, and this documentation is the primary source of current technical information on the TMPA-RT. Huffman et al. (2003) and Huffman et al. (2005) provide earlier short formal summaries (all references are listed in section 13).

.....

## 2. Related Projects, Data Networks, and Data Sets

The \*data set creators\* are G.J. Huffman, D.T. Bolvin, E.J. Nelkin, and R.F. Adler, working in the Mesoscale Atmospheric Processes Laboratory, NASA Goddard Space Flight Center, Code 612, Greenbelt, Maryland, 20771 USA, and E.F. Stocker, working in the Precipitation Processing System (PPS, formerly the TRMM Science Data and Information System, TSDIS), NASA Goddard Space Flight Center, Code 610.2, Greenbelt, Maryland, 20771 USA

.....

The work is being carried out as part of the Tropical Rainfall Measuring Mission (\*TRMM\*), an international project of NASA and JAXA designed to provide improved estimates of precipitation in the Tropics, where the bulk of the Earth's precipitation occurs. TRMM began recording data in December 1997 and ended in April 2015. It flew in a (46-day) precessing orbit at a 35° inclination with a period of about 91.5 min. This orbit allows TRMM to build up a complete view of the climatological diurnal cycle, as well as providing calibration for other precipitation-relevant sensors in Sun-synchronous orbits. The TRMM home page is located at <a href="http://trmm.gsfc.nasa.gov/">http://trmm.gsfc.nasa.gov/</a>.

.....

The TMPA-RT draws on data from several \*data providers\*:

- 1. NASA/GSFC level 1 TMI Tb's (processed with TRMM algorithm 2A12RT at PPS);
- 2. NSIDC Level 2 AMSR-E precipitation estimates (processed with GPROF2004-AMSR at MSFC/GHRC);
- 3. CSU SSMI Level 2 precipitation estimates (processed with GPROF2010 at CSU);
- 4. Navy/FNMOC SDR's of SSMIS Ta's (processed with GPROF2004V-SSMIS at PPS);
- 5. NESDIS/MSPPS operational level 2 AMSU-B precipitation estimates;
- 6. NESDIS/MSPPSoperational level 2 MHS precipitation estimates; and
- 7. NOAA/NWS/CPC Merged 4-Km Geostationary Satellite IR Brightness Temperature Data (processed into VAR at PPS as part of the TMPA-RT).

In addition, climatological calibrations were computed using

- 1. NASA/GSFC level 2 Version 7 TRMM algorithm 2B31 and
- 2. NASA/GSFC level 3 Version 7 TRMM (production) algorithm 3B43.

See "sensors contributing to TMPA-RT" for more details.

Some of these data sets extend beyond the TMPA-RT period in their original archival locations.

.....

There are numerous \*similar data sets\*, although no other matches all the attributes of being routinely produced, publicly available, fine-scale in space and time, quasi-global, near-real-time, intercalibrated, formed by combining multiple data sources, providing multiple combined estimates, and being associated with a research-grade post-real-time product that is similarly processed. The International Precipitation Working Group data set tables, particularly Table 2, at <a href="http://www.isac.cnr.it/~ipwg/data/datasets.html">http://www.isac.cnr.it/~ipwg/data/datasets.html</a> provide a good listing of other precipitation data sets. The closest include the sets of estimates based on:

- Turk (1999), which uses individual SSMI overpasses to calibrate geo-IR precipitation estimates;
- Sorooshian et al. (2000), which applies the PERSIANN neural network to calibrate IR with microwave; and
- Joyce et al. (2004), which applies the CMORPH morphing scheme to time-interpolate microwave patterns with IR-based motion vectors.
- Kubota et al. (2007), which applies the GSMaP morphing scheme to time-interpolate microwave patterns with IR-based motion vectors.
- Huffman et al. (2017), the IMERG data sets, which are the successor to TMPA and TMPA-RT, and will supersede them when retrospectively processed for the TRMM era in Fall 2018.

Several SSMI/SSMIS-based data sets are available as gridded single-sensor data sets with significant data voids in cold-land, snow-covered, and ice-covered areas, including those computed with the GPROF 6.0, 2004a, and 2010 algorithms (based on Kummerow et al. 1996); the NOAA Scattering algorithm (Grody 1991); and the Chang/Chiu/Wilheit emission algorithm (Wilheit et al. 1991, Chiu and Chokngamwong 2010) among others. Other daily, single-sensor data sets are available for open-water regions based on SSMI/SSMIS data (RSS, Wentz and Spencer 1998; HOAPS, Andersson et al. 2010), MSU data (Spencer 1993), AMSR-E, and AMSU-B/MHS data. Several daily single-sensor or combination data sets are available at the regional scale, but are not really "similar."

The Version 7 TRMM product 3B42 is being computed with the TMPA after real time, and constitutes the research-grade archive of TMPA estimates. See "3B42" for details.

.....

The Version 7 TRMM product \*3B42\* is being computed with the TMPA after real time, and constitutes the research-grade archive of TMPA estimates. Note that the version numbering for the TMPA-RT and official TRMM products are not necessarily related, although both are currently numbered 7. The post-real time computation allows several improvements in 3B42 compared to 3B42RT:

- 1. Data are processed starting with the first full month of TRMM data, which begins 1 January 1998.
- 2. The IR calibration period is the calendar month in which the observation time falls, rather than a trailing 30-day accumulation.
- 3. The TRMM Combined Instrument product (2B31) is used as the calibrating standard month-to-month, which should give better estimates than the climatological calibration used in the RT
- 4. For each grid box, the individual 3B42 3-hourly precipitation values are scaled to sum to a combination of monthly 3B42 and gauge analysis, which is TRMM product 3B43.

The first set of reprocessed data for Version 7 were posted in May 2012, while the second was posted in December 2012 (see "additional processing for Version 7"). Product 3B42RT continues to march forward in real time, and 3B42 estimates are considered to supersede the 3B42RT estimates as each month of 3B42 is computed. Note that the RT products take on additional importance during Version 7 due to the increased latency of the official production datasets.

It is planned that both the production and RT TMPA systems will be superseded by Integrated Multi-satellitE Retrievals for GPM (IMERG), although they will continue to be computed until IMERG is considered mature, first in early 2017 for the GPM era and Fall 2018 for the entire TRMM/GPM era. See the section on IMERG for more details.

.....

The \*transition from Version 6 to Version 7\* for TMPA-RT datasets occurred on 25 June 2012. Thereafter, the Precipitation Processing System (PPS) was reconfigured to start the parallel activities of Version 7 RT "initial processing" (IP) for new data (starting 10 May 2012), and Version 7 RT retrospective processing (RP) for the entire archive starting 1 March 2000. This release incorporated several important changes as part of the upgrade to Version 7 RT:

- Retrospective processing during July-September 2012 for the RT system back to 1 March 2000. This satisfies numerous user requests for a long archive of RT data to enable calibration of real-time applications that cannot take advantage of the Version 7 TMPA archive. In this innovative approach the RT code was run on the production computer system, since the RT computer system is not equipped to do such processing. As a result, Version 7 RT data sets will be made available starting 1 March 2000. The main difference from true RT processing is that the full input satellite data sets available in the Version 7 production system are used. These production data archives are somewhat more complete than what would have been received in real time. The start date is driven by the start date of the CPC Merged 4 Km IR data record on 17 February 2000 and the need to spin up the microwave-IR calibration. Retrospectively processed datasets are denoted by the version identifier "7R" in the file name, versus "7" in the "Initial Processing" datasets. It continues to be the case that, despite the long RT record, it is strongly recommended that the production dataset (3B42) be used or all research not specifically focused on RT applications.
- Additional satellites, including the early parts of the various records, the entire operational SSMIS record, and slots for future satellites. But, AMSU and MHS data were accidentally ignored in the first retrospective processing. See "additional processing for Version 7" for more details.

- Uniformly reprocessed input data using current algorithms, most notably for AMSU and MHS, but also including TCI, TMI, AMSR-E, and SSMI.
- Use of Version 7 TCI and 3B43 for (climatological) calibration in 3B42RT.
- Use of a latitude-band calibration scheme for all satellites (see "HQ").

The complete Version 6 archive continues to be maintained for public access. Residual issues with satellite intercalibration, particularly for the early IR data and the SSMIS precipitation estimates, are currently being worked for the TMPA-RT.

Initial testing shows that the V7 TMPA tropical-ocean average precipitation is consistently some 5% higher than the combined TMI-PR product (2B31) that serves as the calibrator. The basis for this difference is not explicated at this point, but the value is small enough and consistent enough that we are choosing to release the data as background work continues. See "intercomparison results" for more details.

.....

Starting with Version 7 the RT system features \*retrospective processing\* to satisfy numerous user requests for a long archive of RT data to enable calibration of real-time applications that cannot take advantage of the Version 7 TMPA archive. In this innovative approach the RT code was run on the production computer system, since the RT computer system is not equipped to do such processing. As a result, RT data sets are available starting 1 March 2000. The main difference from true RT processing is that the full input satellite data sets available in the Version 7 production system are used. These production data archives are somewhat more complete what would have been received in real time. The start date is driven by the start date of the CPC Merged 4 Km IR data record. The current retrospective processing is the second for Version 7, denoted by the version identifier "7R2" in the file name, superseding the original retrospectively processed datasets denoted by "7R" in the file name, and compared to "7" in the "Initial Processing" datasets. See "additional retrospective retrospective processing in Version 7" for more details. It continues to be the case that, despite the long RT record, it is strongly recommended that the production dataset (3B42) be used or all research not specifically focused on RT applications.

.....

An \*additional processing for Version 7\* was carried out when processing issues were discovered with both the Version 7 TMPA production (3B42/43) and Version 7 TMPA-RT (3B40/41/42RT) data series. In general, the original Version 7 data sets are considered an improvement over Version 6, but this additional processing is considered important to meet the goals of the project. Users are urged to switch to the newest Version 7 data sets as soon as practical.

In November 2012 it was discovered that AMSU data were omitted in the first retrospective processing of both the Version 7 TMPA (3B42/43) and TMPA-RT (3B40/41/42RT) data series, which created an important shortcoming in the inventory of microwave precipitation estimates used during 2000-2010. In addition, a coding error in the TMPA-RT replaced the occasional missing-filled areas in product 3B42RT with zero-fills. Accordingly, both product series were retrospectively processed again. The main impact in both series was to improve the fine-scale

patterns of precipitation during the periods noted below, roughly 2000-2010 (3B42/43) and 2000-2012 (3B4xRT). Averages over progressively larger time/space scales should be progressively less affected. [This is the reason the lack of AMSU went undiscovered; the merger system copes very reasonably with missing data.] Nonetheless, users were urged to switch to the newest Version 7 data sets as soon as practical. Subsequently, Yong et al. (2015) pointed out that F16 SSMIS data were also missing in the first retrospective processing.

It should be noted that these retrospective processings were done with archived "production" input data. For the RT, this resulted in some instances in which files that originally had not been received in a timely fashion, and hence did not make it into the original RT product, were ultimately archived when they showed up later, and then were included in the new retrospective processing. As such, the retrospectively processed RT is built from a superset of the data that had actually been available in true real time. The main implication is that the current "Initial Processing" RT being run only on real-time input could have somewhat worse errors than the equivalent reprocessed data.

In the original archive sites the newest runs may be identified by the file name suffixes. Specifically:

- V.7 3B42/43: "7A.HDF" for January 2000 September 2010 on http://mirador.gsfc.nasa.gov/cgi/bin/mirador/presentNavigation.pl?tree=project&project=T RMM&dataGroup=Gridded;
- V.7 3B4xRT: suffix of "7R2.bin" for 00 UTC 1 March 2000 05 UTC 7 November 2012 on ftp://trmmopen.gsfc.nasa.gov/pub/merged/mergeIRMicro/.

However, the secondary archive at *ftp://disc2.nascom.nasa.gov/data/TRMM/Gridded/* associated with Giovanni currently requires a uniform naming convention for each data series. Thus, users must inspect the file date/times to determine that the data are the latest:

- V.7 3B42/43: original retrospectively processed data were posted in late May 2012, the newly reprocessed data (for January 2000 September 2010) were posted in December 2012, and Initial Processing data were posted as produced.
- V.7 3B4xRT: newly reprocessed data (for 00 UTC 1 March 2000 05 UTC 7 November 2012) were posted in January 2013, then Initial Processing data were posted as produced.

In the second retrospective processing it continues to be the case that the Version 7 3B42/43 is some 5-8% higher than the calibrating data set (2B31) over oceans, which is believed to be erroneous. However, the first several attempts at diagnosing this issue have not been fruitful. At the large scales this offset seems to be nearly a proportional constant. Another known issue is that RT over land seems to have an increasing trend that is strongest in south-central Asia and northwestern South America, again for reasons we do not yet understand. The RT trend over land is somewhat weaker in the second retrospective processing.

### .....

# 3. Storage and Distribution Media

The \*data set archive\* consists of unformatted binary files. Each hour or 3-hour dataset is contained in a separate file with a self-documenting ASCII header. The TMPA-RT is distributed

by anonymous FTP over the Internet. Each 3B40RT (3B41RT, 3B42RT) file occupies  $\sim$ 7 (3) MB uncompressed, or  $\sim$ 350 KB (150 KB) compressed.

The full collection of TMPA-RT files are provided and archived on the anonymous FTP sites ftp://trmmopen.gsfc.nasa.gov/pub/merged/ and ftp://trmmopen.gsfc.nasa.gov/pub/TMPA/TRMM realtime/. Other independent sources of these data files exist, but it is highly recommended that users only access the data via the GES DISC as it always has the latest versions of 3B42 and 3B43.

Web-based interactive access to the 3B40RT/41RT/42RT data is provided through Giovanni; see that topic for details.

.....

- 1. Besides the primary data sites (see \*data set archive\*), several "mirror" and value-added archive sites include the TMPA-RT data sets and/or value-added products in their holdings. Users availing themselves of these sites should work with the personnel in charge of those sites to work out access problems. Also, users are urged to gain a clear understanding of the provenance of those data to assure that they are working with current, clean data.
- 2. FTP access is sometimes regulated by the ISP or institution providing Internet connectivity. Specifically, many ISP's and institutions only permit the FTP software on user machines ("clients") to make "passive" FTP connections. At least some Macintosh and Windows native FTP applications default to "active". Users having trouble with FTP access should consult with their computer system support personnel to determine whether this is an issue, and if so, whether shifting to a third-party FTP package is necessary to allow "passive" operation.
- 3. The TMPA-RT data sets are in IEEE "big-endian" floating-point format. Generally Intel-based computers run in "little-endian", meaning the data must be "byte-swapped" to be useful.

.....

\*Giovanni\*, formerly the Geospatial Interactive Online Visualization ANd aNalysis Infrastructure, is created and supported by GES DISC. It provides a web-based resource for accessing many Earth science data sets, including IMERG Runs. It performs a variety of basic subsetting, time- and space-averaging, and output of results in plots, time series, animations, or ASCII text. The current Version 4 of Giovanni is located at

https://giovanni.sci.gsfc.nasa.gov/giovanni/.

#### 4. Reading the Data

A \*data file identifier\* is embedded in the data file name as

<sup>\*</sup>Known data set access issues\* include:

where

product> is the product identifier:

3B40RT = high-quality (HQ) estimate from merged microwave;

3B41RT = variable rainrate (VAR) IR estimate;

3B42RT = combined HQ and VAR.

<datetime> is the nominal UTC date/time as YYYYMMDDHH (i.e., numerical 4-digit year, month, day, hour)

<version> is the processing version

7 = "Initial Processing" (near-real-time processing on the real-time computer system)

7R2 = "Retrospective Processing" (after-the-fact processing on the production computer system)

.....

The \*data file access technique\* is the same for all files. These files are accessible by standard data analysis application programs that support "raw" data access and by programming in third-generation computer languages (FORTRAN, C, etc.).

Each file consists of a 2880-byte header record containing ASCII characters (which is the same size as one 2-byte-integer row of data), then the grid of scaled 2-byte integer precipitation estimates, the grid of scaled 2-byte integer random error estimates, and other 1-byte integer grids. The header line makes the file nearly self-documenting, in particular spelling out the variable and version names, and giving the units of the variables. The header line may be read with standard text editor tools or output under program control. Grid boxes without valid data are filled with the (2-byte integer) "missing" value -31999. The data may be read with standard data-display tools (after skipping the 2880-byte header) or output under program control.

.....

The \*data file layout\* is somewhat different for the different products, as shown in Table 1.

Table 1. File layout for 3B40RT, 3B41RT, 3B42RT.

	3B40RT		<i>3B41RT</i>		<i>3B42RT</i>	
Block	Byte Count	Field	Byte Count	Field	Byte Count	Field
1	2880	header	2880	header	2880	header
2	2073600*	precip	1382400&	precip	1382400&	precip
3	2073600*	error	1382400&	error	1382400&	error
4	1036800+	# pixels	691200@	# pixels	691200@	source
5	1036800+	# ambig. pixels	-	ı	1382400&	uncal precip
6	1036800+	# rain pixels	-	ı	-	-
7	1036800+	source				

<sup>\*</sup> INTEGER\*2, 90°N-S

& INTEGER\*2, 60°N-S

@ INTEGER\*1, 60°N-S

Header:

<sup>+</sup> INTEGER\*1, 90°N-S

Each file starts with a header that is one 2-byte-integer row in length, or 2880 bytes. The header is ASCII in a "PARAMETER=VALUE" format that makes the file self-documenting (e.g., "algorithm\_id=3B40RT"). As such, the header can be read with standard text editors, output as text with simple application programs, or parsed for input into applications. Successive "PARAMETER=VALUE" sets are separated by spaces, and no spaces or "=" are permitted in either PARAMETER or VALUE. The current PARAMETER entries and definitions are:

PARAMETER Definition

algorithm ID TRMM algorithm identifier (e.g., "3B40RT")

algorithm version Version of the science algorithm

granule ID PPS granule identifier (e.g., "3B40RT.2001121809.7R.bin")

header byte length Number of bytes in the header

file structure

nominal YYYYMMDD Nominal UTC year, month, and day of the month

nominal\_HHMMSS Nominal UTC hour, minute, and second begin\_YYYYMMDD Start UTC year, month, and day of the month

begin HHMMSS Start UTC hour, minute, and second

end YYYYMMDD End UTC year, month, and day of the month

end HHMMSS End UTC hour, minute, and second

creation\_YYYYMMDD Date the file was created as year, month, and day of the month

west\_boundary
east\_boundary
north\_boundary
South\_boundary
Longitude of the western edge of the data domain
Latitude of the northern edge of the data domain
Latitude of the southern edge of the data domain

origin Geographical direction of the first grid box from the grid center

number\_of\_latitude\_bins Number of grid boxes in the meridional direction number of longitude bins Number of grid boxes in the zonal direction

grid Size of one grid box

first\_box\_center Geolocation of the first grid box center second\_box\_center Geolocation of the second grid box center last box center Geolocation of the last grid box center

number of variables Number of data fields

variable name List of the data field names, separated by commas

variable units List of data field units, separated by commas, in the same order as

the variable name list

variable\_scale List of data field scaling factors, separated by commas, in the same

order as the variable name list

variable type List of data field word types, separated by commas, in the same

order as the variable name list

byte\_order Order of bytes in a data word ("big\_endian" or "little\_endian")

flag\_value List of special values, separated by commas

flag name List of special value names, separated by commas, in the same order

as the flag value list

contact name Name of the person to contact with questions

contact address Postal address of the contact name

contact\_telephone Telephone number of the contact\_name contact\_facsimile Facsimile number of the contact\_name contact\_email Email address of the contact\_name

Thereafter the data fields follow. All the fields are on a 0.25° lat./lon. grid that increments most rapidly to the east (from the Prime Meridian) and then to the south (from the northern edge). Grid box edges are on multiples of 0.25°. The data fields are written as flat binary data in bigendian byte order.

## 3B40RT:

Following the header, 6 data fields appear:

precipitation (2-byte integer) precipitation\_error (2-byte integer) total\_pixels (1-byte integer)

ambiguous pixels (1-byte integer; highly uncertain values)

rain pixels (1-byte integer)

source (1-byte integer; the values are:

0 = no observation 1 = AMSU 2 = TMI

3 = AMSR 4 = SSMI 5 = F17 SSMIS 6 = MHS 7 = MetOp-B 8 = spare sounder 29 = spare sounder 3 10 = F16 SSMIS 11 = F18 SSMIS

12 = spare scanner 6 30 = AMSU&MHS avg.

31 = conical avg. 1,2,...,12 + 100 = sparse-sample HQ)

All fields are 1440x720 grid boxes (0-360°E,90°N-S). The first grid box center is at (0.125°E,89.875°N). Files are produced every 3 hours on synoptic observation hours (00, 03, ..., 21 UTC) as an accumulation of all HQ swath data observed within +/-90 minutes of the nominal file time. Estimates are only computed for the band 70°N-S.

Note that for historical reasons the source field coding is slightly different than for the production TMPA.

### 3B41RT:

Following the header, 3 data fields appear:

precipitation (2-byte integer) precipitation\_error (2-byte integer) total\_pixels (1-byte integer)

All fields are 1440x480 grid boxes (0-360°E,60°N-S). The first grid box center is at (0.125°E,59.875°N). Files are produced every hour from the on-hour IR image (except for the previous half-hour image for GMS), with fill-in by the previous half-hour image (except for GMS, where the on-hour image is used for fill-in). Valid estimates are only provided in the band 50°N-S.

#### 3B42RT:

```
Following the header, 4 data fields appear:
  precipitation
                      (2-byte integer)
  precipitation error (2-byte integer)
                      (1-byte integer; the values are:
  source
                      0 = no observation
                                             1 = AMSU
                                                                    2 = TMI
                      3 = AMSR
                                             4 = SSMI
                                                                    5 = F17 SSMIS
                                                                    8 = \text{spare sounder } 2
                      6 = MHS
                                             7 = MetOp-B
                      9 = spare sounder 3
                                             10 = F16 SSMIS
                                                                    11 = F18 SSMIS
                      12 = \text{spare scanner } 6 30 = \text{AMSU\&MHS avg.}
                      31 = conical avg.
                                             50 = IR
                      1,2,...,12 + 100 = sparse-sample HQ)
                      (2-byte integer)
uncal. Precip
```

Note that for historical reasons the source field coding is slightly different than for the production TMPA.

All fields are 1440x480 grid boxes (0-360°E,60°N-S). The first grid box center is at (0.125°E,59.875°N). Files are produced every 3 hours on synoptic observation hours (00, 03, ..., 21 UTC) using that hour's 3B40RT and 3B41RT data sets. Valid estimates are only provided in the band 50°N-S. See "decode high-latitude VAR and HQ+VAR precipitation values" for discussion of retrieving values outside 50°N-S. The leading precipitation field has a climatological bias correction to the 3B42 Version 7 estimates (see step 2 in "HQ+VAR", 3B42RT), while the last field is the multi-satellite precipitation before this calibration.

Note that we use the term "gridbox" to denote the values on Level 3 data (i.e., gridded data), while we use the term "pixel" to denote individual values of Level 2 data (i.e., instrument footprints). Thus, there can be many pixels contributing to a gridbox.

Both precipitation and random error are scaled by 100 before conversion to 2-byte integer. Thus, units are 0.01 mm/h. To recover the original floating-point values in mm/h, divide by 100. Missings are given the 2-byte-integer missing value, -31999. The remaining fields are in numbers of pixels, except the source variable, which is dimensionless.

Currently the random error fields are all set to the 2-byte-integer missing value, -31999. This placeholder will be replaced with actual estimates as development proceeds.

The variable ambiguous\_pixels is the count of pixels for which the algorithm cannot determine whether the scene has valid or invalid data. It is a subset of the total\_pixel and many, but not all, are included in raining\_pixels. In general, a "high" fraction of ambiguous\_pixels indicates that the grid box value is invalid.

The data are written as "big-endian" IEEE 754-1985 representation of 4-byte floating-point unformatted binary numbers. Some CPUs, including PCs and Linux machines, might require a

change of representation (i.e., byte swapping) before using the data. In some cases, the gunzip routine, used to uncompress the data, will change representations automatically.

.....

The \*originating machine\* on which the data files were computed is a Linux workstation, which uses the "little-endian" representation of unformatted binary words, but for continuity with past versions the data are posted in "big-endian" representation. Some CPUs, such as PCs and Linux machines, might require a change of representation (i.e., byte swapping) before using the data.

.....

It is possible to \*read the header record\* with most text editor tools, although the size (2880 bytes) may be longer than some tools will support. Alternatively, the header record may be output under program control, as demonstrated in "Read the Header Record FORTRAN Example" in the Appendices. The header is written in a "PARAMETER=VALUE" format documented in "data file layout," where PARAMETER is a string without embedded blanks that gives the parameter name, VALUE is a string that gives the value of the parameter, and blanks separate each "PARAMETER=VALUE" set. To prevent ambiguity, no spaces or "=" are permitted as characters in either PARAMETER or VALUE.

See "Read the Header Record, FORTRAN Example" in the Appendices for specifics.

.....

It is possible to \*read a file of data\* with many standard data-display tools. The 2880-byte header is designed to be exactly the size of one row of data, so the header may be bypassed by skipping 2880 bytes or 1440 2-byte integer data points or one row. Alternatively, the data may be output under program control as demonstrated in the "Read a File of Data" example programs in the Appendices. Once past the header, there are always a precipitation field, a random error field, and 1-5 auxiliary fields. As documented in "Data File Layout", the grids are either 1440x720 (3B40RT) or 1440x480 (3B41RT, 3B42RT) and the data are either scaled 2-byte integer (precipitation, random error, and uncalibrated precipitation) or 1-byte integer (all others). Grid boxes without valid data are filled with the "missing" value -31999 for 2-byte integer fields and 0 for 1-byte integer fields.

See the "Read a File of Data" examples in the Appendices for specifics.

.....

It is possible to \*decode high-latitude VAR and HQ+VAR precipitation values\* with

$$p = -0.01 * (v + 1)$$

where p is the floating-point value,

v is the scaled-integer value, and

v is not equal to the 2-byte-integer missing value (-31999).

This encoding is done because the data set developers consider the high-latitude values to be very unreliable, but they wish to have the values available for data set development work and special data-set user needs.

.....

It is possible to \*decode highly ambiguous HQ values\* with

$$p = -0.01 * (v + 1)$$

where p is the floating-point value,

v is the scaled-integer value, and

v is not equal to the 2-byte-integer missing value (-31999).

This encoding is done because it is likely that HQ values with a large fraction of pixels flagged as "ambiguous" contain artifacts. However, the full population of ambiguous pixels must be available to subsequent processing for the VAR calibration, so these values are not set to "missing" until they are combined with VAR to create HQ+VAR (3B42RT). See "ambiguous pixels" for more details.

.....

# 5. Definitions and Defining Algorithms

The \*precipitation variable\* is computed as described under the individual product headings. All precipitation products have been converted from their original units to mm/h. Throughout this document, "precipitation" refers to all forms of precipitation, including rain, drizzle, snow, graupel, and hail (see \*precipitation phase\*).

.....

The \*precipitation phase\* is not explicitly treated by the TMPA-RT or its input datasets. The algorithms sense total hydrometeor mass in the atmospheric column (except the passive microwave retrievals only consider total solid hydrometeor mass over land and coast. Also, note that the passive microwave algorithms cannot retrieve any precipitation over a snowy/icy surface, regardless of the phase of the surface precipitation, although it is generally snow. The IR retrievals are calibrated to the passive microwave retrievals, again, without reference to precipitation phase. These IR calibrations are in-filled from surrounding areas in the snowy/icy-surface areas where microwave cannot provide estimates. Given these facts, the "precipitation" reported in this document refers to all forms of precipitation, including rain, drizzle, snow, graupel, and hail.

.....

The \*time zone\* for this data set is Universal Coordinated Time (UTC, also known as GMT or Z).

Because the data are provided at nominal UTC hours, each data set represents a nominal +/-30-minute (90-minute) span around the nominal hour for 3B41RT (3B40RT, 3B42RT). Thus, the 00 UTC images include data from the very end of the previous UTC day.

.....

The \*Merged 4-Km IR Tb data set\* is produced by the Climate Prediction Center (CPC), NOAA National Centers for Environmental Prediction, Washington, DC under the direction of P. Xie. Each cooperating geostationary (geo) satellite operator (the Geosynchronous Operational Environmental Satellites [GOES], United States; the Geosynchronous Meteorological Satellite [GMS], followed by the Multi-functional Transport Satellite [ and then Himawari 8], Japan; and the Meteorological Satellite [Meteosat], European Community) forwards infrared (IR) imagery to CPC. Then global geo-IR are zenith-angle corrected (Joyce et al. 2001), re-navigated for parallax, and merged on a global grid. In the event of duplicate data in a grid box, the value with the smaller zenith angle is taken. The data are provided on a 4-km-equivalent latitude/longitude grid over the latitude band 60°N-S, with a total grid size of 9896x3298.

The data set was first produced in late 1999, but the current uniformly processed record is available starting 17 February 2000. CPC is working to extend the record back to January 1998.

All 5 geo-IR satellites are used, with essentially continuous coverage. GMS-5 was replaced by GOES-9 starting 01 UTC 22 May 2003, which introduced slightly different instrument characteristics. Then starting 19 UTC 17 November 2005 the new Japanese MTSat-1R took over, followed by MTSat-2 on 1July 2010, and then Himawari 8 at 02 UTC on 7 July 2015.

Each UTC hour file contains 2 data fields. All geo-IR images with start times within 15 minutes of the UTC hour are accumulated in the "on-hour" field. Images with start times within 15 minutes of the UTC hour plus 30 minutes are accumulated in the "half-hour" field. The nominal image start times for the various satellites and their assignment to half-hour fields are shown in Table 2.

Table 2. Nominal sub-satellite longitude (in degrees longitude) and image start time (in minutes past the hour) for the various geosynchronous satellites. The start times are displayed according to their assignment to either the on-hour or half-hour fields in the CPC Merged 4-Km IR Tb data set. Full-disc views are guaranteed only at 00, 03, ..., 21 UTC. These appear in the on-hour field except the Japanese satellite appears in the previous half-hour for all hours. For images not at these times, a satellite's "image" may be assembled from various operator-specified regional sectors. The Japanese satellite provides N. Hemisphere sectors (only) on-hour, except S. Hemisphere sectors (only) at 00, 06, 12, 18 UTC.

Satellite	Sub-sat. Lon.	on-hour	half-hour
GMS, MTSat, Himawari	140°E	00	30
series			
GOES-E (8, 12, 13, now 16)	75°W	45	15
GOES-W (10, 11, now 15)	135°W	00	30
Meteosat-11 (formerly 5, 7, 8,	0°E	00	30
9, 10)			
Meteosat-8 (formerly 5, 7)	41.5°E	00	30
	$(63^{\circ}\text{E for } 5, 7)$		

These data are used as input to TMPA-RT processing.

.....

The Goddard Profiling Algorithm (\*GPROF\*) is based on Kummerow et al. (1996) and Olson et al. (1999). GPROF is a multi-channel physical approach for retrieving precipitation and vertical structure information from satellite-based passive microwave observations (here, TMI, AMSR-E, SSMI and SSMIS). The GPROF-AMSR-E, GPROF-SSMI, and GPROF-SSMIS estimates are computed from their respective Tb's as part of the TMPA-RT, while the GPROF-TMI estimates are computed by PPS as 2A12RT. GPROF applies a Bayesian inversion method to the observed microwave brightness temperatures using an extensive library of profiles relating hydrometeor profiles, microwave brightness temperatures, and surface precipitation rates. The GPROF 2004 library depends on cloud model computations, while the GPROF2010 library is based on PR data. GPROF includes a procedure that accounts for inhomogeneities of the rainfall within the satellite field of view. Over land and coastal surface areas the algorithm reduces to a scattering-type procedure using only the higher-frequency channels. This loss of information arises from the physics of the emission signal in the lower frequencies when the underlying surface is other than all water.

Various versions of this algorithm are applied to the TMI, AMSR-E, SSMI, and SSMIS Tb data, and the estimates are used as input to TMPA processing. At the time Version 7 began, the most current GPROF was GPROF2010. The TMI estimates are computed using GPROF-TMI Version 7 (GPROF2010). All AMSR-E estimates have been computed using Version 10/11 of GPROF-AMSR (GPROF2004). The SSMI estimates are computed using GPROF2010-SSMI.

The SSMIS estimates are computed with a modification of GPROF2004 by D. Vila (which we have named GPROF2004v; Vila et al. 2013) that accounts for navigation and scan-strategy differences, calibrates the Ta's for all channels to approximate the behavior of coincident SSMI Ta's, and develops 85-GHz proxy channels from the SSMIS 91 GHz channels. The calibration to SSMI first applies "scan correction coefficients" to each of the SSMIS channels, which adjust the Ta value by a scale factor that is very close to 1.0, but which varies by field of view. This has to do with achieving scan uniformity, because the Ta values tend to drop off at the edge of the scan. Second, a histogram match is applied to the Ta's, dependent on surface type, to make the SSMIS values look like SSMI. This is done separately for the 19, 22, 37, and 91 GHz Ta's. Finally, there is a Ta-to-Tb conversion (presumably the one used in NESDIS to do the conversion for SSMI).

.....

PPS algorithm \*2A12RT\* contains level 2 (scan-pixel) GPROF estimates of precipitation based on TMI data. These are provided by PPS, led by Erich Stocker. Each file contains an orbit of estimates. The data have had some quality control, and are converted from sensor units to Ta, then to Tb, then to precipitation.

These data are used as input to TMPA-RT processing.

.....

<sup>\*</sup>SSMI Level 2 precipitation estimates\* are those produced by Colorado State University.

These estimates are computed on Level 1c SSMI brightness temperatures using GPROF 2010. Level 1c is defined as Level 1b with (potentially) different calibrations applied than the original source.

.....

\*SSMIS Level 1b Ta data\* are those produced by Fleet Numerical Meteorological and Oceanographic Center, Monterey, CA.

These data are used as input to GPROF2004v-SSMIS, which was developed as modifications to GPROF2004 by D. Vila (which we therefore named GPROF2004v; Vila et al. 2013) and further modified to run at PPS (see "GPROF").

.....

PPS algorithm \*2B31\* contains Level 2 (scan-pixel) output from the Version 7 combined PR-TMI retrieval algorithm, computed at PPS. The TRMM Combined Algorithm (TCI) combines data from the TMI and PR to produce the best rain estimate for TRMM. Currently, it uses the low frequency channels of TMI to find the total path attenuation. This information is used to constrain the radar equation. Each file contains an orbit of TCI rain rate and path-integrated attenuation at 4 km horizontal and 250 m vertical resolutions over a 220 km swath. More information is available at

 ${\it http://disc.gsfc.nasa.gov/precipitation/TRMM\_README/TRMM\_2B31\_readme.shtml}$ 

and Haddad et al. (1997a,b).

These Level 2 data are used as input to TMPA processing. Although not directly relevant to the RT system, not that production ended in early October 2014 when fuel exhaustion allowed TRMM to descend below the orbital altitude where the fixed range bins for the PR usefully saw near-surface data.

.....

The \*AMSU-B precipitation data set\* is computed operationally at the National Environmental Satellite Data and Information Service (NESDIS) Microwave Surface and Precipitation Products System (MSPPS) based on the Zhao and Weng (2002) and Weng et al. (2003) algorithm. Ice water path (IWP) and particle effective diameter size (De) are computed from the 89 and 150 GHz channels. As such, it is a primarily a scattering approach. Surface screening is carried out using Advanced Very High Resolution Radiometer (AVHRR) infrared data and Global Data Assimilation System (GDAS) surface temperature and surface type data to discriminate desert, snowy, or icy surfaces. Precipitation rate is computed based on IWP—precipitation rate relations derived from the NCAR/PSU Mesoscale Model Version 5 (MM5). The precipitation rate is approximated as a second-degree polynomial in IWP, with coefficients that are derived separately for convective and non-convective situations, based upon a series of comparisons between the three AMSU-B channels centered at the 183.31 GHz water vapor absorption band. Additionally, the algorithm identifies regions of falling snow over land through the use of

AMSU-A measurements at 53.8 GHz. At present, falling snow is assigned a rate of 0.1 mm/hr, although an experimental snowfall rate is being tested and evaluated.

The data set was first produced in early 2000. The algorithm was last upgraded on 31 May 2007 and subsequently reprocessed. In the latter, an emission component was added to increase the areal coverage of precipitation over oceans through the use of a liquid water estimation using AMSU-A 23.8 and 31 GHz (Vila et al. 2007). Additionally, an improved coastline precipitation rate module was added that computes a proxy IWP using the 183 GHz bands (Kongoli et al. 2007). As a result, oceanic precipitation estimates in Version 7 are improved over Version 6 for the period 2000-2007.

These level	2 data are u	ised as input to	TMPA-RT	processing

The \*MHS precipitation data set\* is computed operationally at the National Environmental Satellite Data and Information Service (NESDIS) Microwave Surface and Precipitation Products System (MSPPS) based on the algorithm previously developed to compute the AMSU-B precipitation data set (which see for details). The channel differences between the sensors are accounted for by computing synthetic 150 and 183±7 GHz channels before the precipitation is computed.

These 1	Level 2	data are	e used	as	input to	TMPA	-RT	process	ing.

The High Quality (\*HQ\*) combined microwave precipitation estimate provides an 0.25°x0.25°-averaged 3-hourly combination of all available TMI, AMSR-E, SSMI, SSMIS, AMSU-B, and MHS estimates:

- 1. The GPROF-AMSR, GPROF-SSMI, GPROF-SSMIS, AMSU-B, MHS, and 2A12RT estimates are gridded to a 0.25°x0.25° grid for a 3-hour period centered on the major synoptic times (00, 03, ..., 21 UTC). The 2A12 data are thresholded at 0.1 mm/hr to control excessive occurrence of precipitation. All of the following steps are carried out with these gridded fields.
- 2. Offline, the GPROF-AMSR, GPROF-SSMI, GPROF-SSMIS, AMSU-B, and MHS have been climatologically probability-matched to 2A12RT. The calibrations of AMSU-B, MHS, SSMI, SSMIS, and AMSR-E to TMI each have one set of coefficients for each sensor type for land and 14 sets for ocean, while SSMIS is calibrated separately for each satellite, again having one set for land and 14 for ocean. The ocean latitude bands are 15° overlapping latitude bands centered on the 5° bands 35-30°S, 30-25°S, 25-20°S, ..., 20-25°N, 25-30°N, and 30-35°N. The outermost bands are used in their respective hemispheres for all higher-latitude calibrations due to the lack of TMI data beyond about 38°. The SSMIS are calibrated individually due to particular calibration issues for each satellite. AMSR-E uses a 2-month set of match-ups to ensure sufficient sampling, while all of the others work with single-month accumulations. The coefficients are computed separately for each season. Finally, a volume adjustment factor is computed for each set to ensure that total TMI precipitation is preserved in these transformations.

- 3. The GPROF-AMSR, GPROF-SSMI, GPROF-SSMIS, AMSU-B, and MHS estimates are climatologically calibrated to 2A12RT.
- 4. The precipitation rate in each grid box is the pixel-weighted average of the calibrated conical-scan microwave radiometer estimates (2A12RT, GPROF-AMSR, GPROF-SSMI, and GPROF-SSMIS) contributing during the 3 hours, or the pixel-weighted average of AMSU-B and MHS if no other HQ estimates are available. Most of the time there's only one overpass some time during the dataset's 3-hour window of whatever the "best" type of sensor is, and so the value is generally one snapshot spatially averaged over the grid box. As an aside, the histogram of rain rates is sensitive to averaging one, two, or three overpasses in a 3-hour period, so in IMERG we will be using only the "best" sensor closest to the mid-point of the IMERG time window (30 minutes). As noted below in HQ+VAR, if no HQ is available, the final combined estimate is given the single IR snapshot estimate at the nominal (i.e., center) time of the dataset.
- 5. Additional fields in the data file include the number of pixels, the number of pixels with non-zero precipitation, the number of pixels for which the estimate is "ambiguous," or highly uncertain, and the sensor type providing the estimate.
- 6. All of the HQ algorithms are unable to provide estimates in regions with frozen or icy surfaces.
- 7. In a future upgrade the random error will be estimated. Currently the random error field is set to missing.

These data are output as 3B40RT in TMPA-RT processing.
*3B40RT* is the official PPS identifier of the HQ data set. The identifier indicates that it is level 3 (gridded) product with input from multiple sensors ("B") using non-TRMM data ("40" series), running in Real Time.

The Variable Rainrate (\**VAR*\*) IR precipitation estimate converts 0.25°x0.25°-averaged geo-IR Tb to precipitation rates that are HQ-calibrated locally in time and space:

- 1. Both geo-IR Tb and HQ are averaged to a 0.25°x0.25° to ensure consistent spatial scale, and time-space matched data are accumulated over pentads (5-day period).
- 2. The computation is done every 3 hr on match-ups contained in the 5 previous pentads, plus whatever part of the current pentad has been observed.
- 3. In each calibration, the Tb-precipitation rate curve is set locally by probability matching the trailing ~30-day histograms of coincident IR Tb and HQ precipitation rate.

In parallel, the current VAR Tb-precipitation rate curve is applied to each Merged 4-Km IR Tb data set as it becomes available:

1. Over most of the globe the on-hour data field is taken as the input data, with fill-in by the previous half-hour image. The exception is the GMS sector, where the previous half-hour is primary, since GMS does not schedule images on the hour. [In that case, much of the GMS sector is filled with data from METEOSAT5 and GOES-W at very high zenith angles.]

- 2. The Tb-to-precipitation rate conversion is a simple look-up, using whatever set of VAR calibration coefficients is current.
- 3. The additional field in the file is the number of pixels.
- 4. The IR estimates are available in the latitude band 60°N-S, but values outside the band 50°N-S are encoded to negative because they are considered highly uncertain. Accordingly, users generally should not employ these values.
- 5. In a future upgrade the random error will be estimated. Currently the random error field is set to missing.

These data are output as 3B41RT in TMPA-RT processing.
*3B41RT* is the official PPS identifier of the VAR data set. The identifier indicates that it is a level 3 (gridded) product with input from multiple sensors ("B") using non-TRMM data ("40" series), running in Real Time.

The combination of \*HQ+VAR\* is computed every 3 hours from that hour's HQ and VAR fields. See Huffman et al. (2010) for a discussion.

- 1. The present combination scheme is to take the HQ field wherever it is non-missing, and fill in with the single-snapshot VAR at the nominal datafile time elsewhere.
- 2. Offline, 14 years of matched instantaneous TCI and TMI have been used to compute climatological monthly calibration histograms, working with 0.25° grid values accumulated on a 1°x1° grid smoothed with a 3x3 moving boxcar template. As well, 14 years of monthly TCI and 3B43 Version 7 estimates have been used to compute climatological monthly calibration ratios, starting with 0.5° averages, smoothing the TCI with a 5x5 moving boxcar template, and averaging both to 1°. For both steps, the statistics are smooth-filled over 36-40° N and S (just outside the TCI zone), and then the 40° N and S values are extended to all higher latitudes using a smooth-fill scheme. In use, the TMI-TCI and TCI-3B43 calibrations are applied sequentially to the initial 3-hourly HQ+VAR fields.
- 3. The additional fields in the file are the source of the estimate and the uncalibrated HQ+VAR estimate.
- 4. The VAR estimates are only trusted for the latitude band 50°N-S, so both the calibrated and uncalibrated HQ+VAR fields are clipped to 50°N-S, with estimates outside that encoded to negative values. Accordingly, users generally should not employ these values.
- 5. It is planned to do a more sophisticated combination in a future release.
- 6. In a future upgrade the random error will be estimated. Currently the random error field is set to missing.

These data are output as 3B42RT in TMPA-RT processing.	

<sup>\*3</sup>B42RT\* is the official PPS identifier of the HQ+VAR data set. The identifier indicates that it is a level 3 (gridded) product with input from multiple sensors ("B") using non-TRMM data ("40"-series), running in Real Time.

.....

The \*units of the TMPA-RT estimates\* as stored in the data files is 0.01 mm/h for both precipitation and random error. To recover the original floating-point values in mm/h, divide by 100. The precipitation values are based on satellite snapshots. These might be thought of as an instantaneous rate, valid at the nominal observation time, although Villarini and Krajewski (2007) showed that 3B42 is best correlated with radar data averaged over 60-90 minutes, not always centered on the nominal overpass time. Missings are given the 2-byte-integer missing value, -31999. The remaining fields are in numbers of pixels, except the source variable, which is dimensionless.

.....

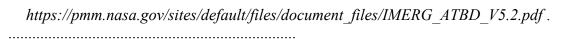
The Merged Multi-satelliE Retrievals for GPM (\*IMERG\*) is being developed as a unified U.S. algorithm for the Day-1 multi-satellite precipitation product by the U.S. GPM team. The precipitation estimates computed from the various precipitation-relevant satellite passive Microwave (PMW) sensors are using GPROF2017 computed at the Precipitation Processing System (PPS) as is now done for the TRMM Multi-satellite Precipitation Analysis (TMPA). These estimates are gridded and intercalibrated, then combined into half-hourly fields and provided to both the Climate Prediction Center (CPC) Morphing-Kalman Filter (CMORPH-KF) Lagrangian time interpolation scheme and the Precipitation Estimation from Remotely Sensed Information using Artificial Neural Networks – Cloud Classification System (PERSIANN-CCS) re-calibration scheme. In parallel, CPC assembles the zenith-angle-corrected, intercalibrated "even-odd" geo-IR fields and forward them to PPS for use in the CMORPH-KF Lagrangian time interpolation scheme and the PERSIANN-CCS computation routines. The PERSIANN-CCS estimates are computed (supported by an asynchronous re-calibration cycle) and sent to the CMORPH-KF Lagrangian time interpolation scheme. The CMORPH-KF Lagrangian time interpolation (supported by an asynchronous KF weights updating cycle) uses the PMW and IR estimates to create half-hourly estimates. The system will be run twice in near-real time

- "Early" multi-satellite product ~4 hr after observation time and
- "Late" multi-satellite product ~14 hr after observation time,

and once after the monthly gauge analysis is received

• "Final" satellite-gauge product ~3 months after the observation month.

The baseline is for the (near-)real-time "Early" and "Late" estimates to be calibrated with climatological coefficients that vary by month and location, while in the "Final" post-real-time run the multi-satellite estimates are adjusted so that they sum to a monthly satellite-gauge combination following the TMPA. In all cases the output contains multiple fields that provide information on the input data, selected intermediate fields, and estimation quality. For more details see the IMERG ATBD (Huffman et al. 2017), posted at



### 6. Temporal and Spatial Coverage and Resolution

The \*file date\* is the UTC year, month, day in which the nominal time of the data set occurs. All dates are UTC.

.....

The \*temporal resolution\* of the products varies:

3B40RT is 3 hr

3B41RT is 1 hr

3B42RT is 3 hr

The 3-hour period is driven by the need for the HQ to accumulate a reasonable sample without encompassing too large a fraction of the diurnal cycle. Note that both the microwave and IR data are instantaneous, except for small regions in which 2 (or more) overlapping microwave scenes are averaged in the HQ field (3B40RT, used in 3B42RT). This is done to make the statistics of the data sets as comparable as possible. The precipitation values are based on satellite snapshots. These might be thought of as an instantaneous rate, valid at the nominal observation time, although Villarini and Krajewski (2007) showed that 3B42 is best correlated with radar data averaged over 60-90 minutes, not always centered on the nominal overpass time.

.....

The \*period of record\* for the TMPA-RT is 1 March 2000 through the present. The start is based on the start of the CPC merged 4 Km IR Tb data set. In contrast, the Version 7 TRMM product 3B42 provides after-real-time processing of the TMPA from 1 January 1998 to the delayed present. See "3B42" for more details.

Data produced with early versions of the TMPA-RT (up to 3 February 2005) are considered obsolete and should not be used. Subsequent Version 5 and 6 data up through 25 June 2012 have reasonable continuity with the current processing system's output, but lack the current calibration and additional satellites. The first retrospective processing constituted a significant advance in consistency, despite the detects outlined in "additional processing for Version 7", but users are urged to use the current dataset. In all cases, users are urged to work with the Version 7 TMPA research product whenever the focus is not specifically real-time operations.

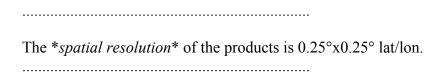
.....

The \*grid\* on which each field of values is presented is a 0.25°x0.25° latitude--longitude (Cylindrical Equal Distance) global array of points. It is size 1440x720 (3B40RT) or 1440x480 (3B41RT, 3B42RT), with X (longitude) incrementing most rapidly West to East from the Prime Meridian, and then Y (latitude) incrementing North to South from the northern edge. Quarter-degree latitude and longitude values are at grid edges.

*Table 3. Representative gridbox center locations for TMPA-RT products.* 

Location	3B40RT	<i>3B41RT,3B42RT</i>
First point center	89.875°N,0.125°E	59.875°N,0.125°E
Second point center	89.875°N,0.375°E	59.875°N,0.375°E
Last point center	89.875°S,0.125°W	59.875°S,0.125°W

The reference datum is WGS84.



The \*spatial coverage\* of the products varies:

*Table 4. Spatial coverage of TMPA-RT products.* 

- 11010 11					
Product	Grid coverage	Maximum extent of data			
3B40RT	90°N-S	70°N-S			
3B41RT	60°N-S	50°N-S (encoded negative at higher lat)			
3B42RT	60°N-S	50°N-S (encoded negative at higher lat)			

.....

# 7. Production and Updates

\*Production and updates\* for the TMPA-RT are a joint activity of the precipitation research group in NASA Goddard Space Flight Center in the Mesoscale Atmospheric Processes Laboratory and PPS.

The latency of the products after observation time is governed by the latency of the individual input products. At this time the pacing item is the delivery of all NOAA-18 MHS granules that contain data for a given HQ file. Because the "contact" needed to get the last few minutes of a 3-hour HQ window may contain up to 2 orbits, the HQ production job is set to run some 7 hours past the nominal hour. Once initiated, the processing occurs in a matter of minutes.

Updates will be released to (1) extend the data record, (2) take advantage of improved combination techniques, or (3) correct errors. Updates resulting from the last two cases will be given new version numbers.

NOTE: The changes described in this section are typical of the changes that are required to keep the TMPA-RT abreast of current requirements and science. Users are strongly encouraged to check back routinely for additional upgrades and to refer other users to this site rather than redistributing data that are potentially out of date.

The TRMM satellite was boosted from an altitude of 350 km to 401.5 km over the period 7-14 August 2001 to lengthen the life of the mission, in fact more than doubling it. This change slightly degraded the instrument resolution. Subsequently, the various algorithms were modified to account for as many of the effects as possible, although residuals are noticeable in some cases.

In some cases, such as the failure of AMSR-E, the end of a data record is clear. In other cases, such as the gradual failure of the NOAA-16 AMSU-B during 2010, the point at which to end use of the data is a matter of judgment. In the latter case we chose 30 April 2010 for Version 7 despite continued operation into early 2011.

As described in "additional processing for Version 7", the initial retrospective processing accidentally omitted AMSU and MHS data, as well as filling 3B42RT missings with zeros. As a

result, an immediate retrospective processing was carried out without a change in version number, although the version identifier contained in file names from the retrospective part of the processing is now "7R2" instead of "7R".

As described in "TRMM end of mission issues", the calibration to 2B31 for TMPA V7 shifted from using coincident data to a climatological calibration as of October 2014, but this didn't affect TMPA-RT

In the future,	all products w	ill be provided	with random	error estimates.

Several \*TRMM end of mission issues\* impact the TMPA 3B42/43 and RT systems:

- 1. On 7 October 2014, routine production ended for the TRMM PR precipitation estimates due to the ongoing descent and ultimate decommissioning of the TRMM satellite (PMM, 2014). [PR data were briefly available from 12 February to 1 April 2015 as TRMM descended past its original altitude of 350 km, but were not used in TMPA.] Estimates from the TMI continued to be produced until it was turned off on 8 April 2015 as part of the TRMM decommissioning. Since PR was no longer available, the TCI estimates are also no longer available. As the research version of the TMPA (products 3B42 and 3B43) uses the TCI estimates as the satellite calibrator, September 2014 was the last month these products were produced in this way. Note that the real-time TMPA (TMPA-RT – products 3B40RT, 3B41RT and 3B42RT) uses climatological satellite calibrations, so continues despite the loss of TRMM estimates. In an effort to keep the research version of TMPA available and usable, we adapted the TMPA-RT climatological calibrations/adjustments for use in the research products. October 2014 is the first month of the climatologically calibrated/adjusted research TMPA. Users should note there will be a discontinuity in the research TMPA record as a result, the degree of which will be provided by analysis of test results generated for the period October 2013 – September 2014. These months of test data can be provided to users upon request. Each individual user must determine the most appropriate use of the climatologically calibrated/adjusted 3B42 and 3B43 products, based on the comparison results provided below and the user's own analysis. We encourage users to report their findings to the developers for the benefit of the community.
- 2. TMI continued to be included as one of the input data sets until it was ended on 8 April 2015 as part of the TRMM decommissioning activities.
- 3. Despite the end of TRMM operations, the successor IMERG will not be a complete replacement until retrospective processing is carried out in Fall 2018. Giving a decent interval for users to make the transition argues for continuing TMPA production until late 2018.

#### 8. Sensors

The TRMM Microwave Imager (\**TMI*\*) is a multi-channel passive microwave radiometer that flies on TRMM. TRMM is placed in a (46-day) precessing orbit at a 35° inclination with a period of about 91.5 min. The channels have effective fields of view that vary from 4.6x6.9 km for the 85 GHz (oval due to the slanted viewing angle) to 29.1x55.2 km for the 10 GHz.

Consequently, the 85 GHz is undersampled, and all other channels are more or less oversampled. At the swath edge even the 85.5 GHz is oversampled.

The TMI is an operational sensor, so the data record suffers the usual gaps in the record due to processing errors, down time on receivers, etc. There were outages for an operational anomaly in May 2000, and the boost to a higher orbit during the first part of August 2001. As summarized in "TRMM end of mission issues", regular computation of TMI data ended on 8 April 2015.

The 35° inclination provides nominal coverage over the latitudes 40°N-S, although limitations in retrieval techniques prevent useful precipitation estimates in cases of cold land or sea ice (if there happened to be any).

Further d	letails a	are availa	able ir	ı Kummer	ow et al.	(1998).

The Advanced Microwave Scanning Radiometer for the Earth Observing System (\*AMSR-E\*) is a multi-channel passive microwave radiometer provided by the Japan Aerospace Exploration Agency that has flown on Aqua from mid-2003 until it failed in late 2011. Data used in the TMPA-RT cover 1 April 2004 – 3 October 2011. Aqua is placed in a sun-synchronous polar orbit with a period of about 102 min. The AMSR-E provides vertical and horizontal polarization values for 6, 10, 18, 23, 36, and 89 GHz frequencies (except only vertical at 23) with conical scanning, similar to the SSMI. Pixels and scans are spaced 10 km apart at the suborbital point, except the 85-GHz channels are collected at 5 km spacing. However, the B-scan sensor, which provides the 89 GHz scan between the lower-frequency scans, failed around 4 November 2004. Every other high-frequency pixel is co-located with the low-frequency pixels, starting with the first pixel in the scan and the first scan in a pair of scans. The channels have resolutions that vary from 4x6 km for the 89 GHz (oval due to the slanted viewing angle) to 43x74 km for the 6 GHz.

The polar orbit provides nominal coverage over the latitudes 85°N-S, although limitations in current retrieval techniques prevent useful precipitation estimates in cases of cold land or sea ice.

The AMSR-E is an operational sensor, so the data record suffers the usual gaps in the record due to processing errors, down time on receivers, etc. Over time the coverage has improved as the operational system has matured. As noted above, the B-scan sensor failed around 4 November 2004.

Further	details ar	e available at	http://www	.ghcc.msfc.nas	a.gov/AMSR/.

The Special Sensor Microwave/Imager (\*SSMI\*) is a multi-channel passive microwave radiometer that has flown on selected Defense Meteorological Satellite Program (DMSP) platforms since mid-1987. The DMSP is placed in a sun-synchronous polar orbit with a period of about 102 min. The SSMI provides vertical and horizontal polarization values for 19, 22, 37, and 85 GHz frequencies (except only vertical at 22) with conical scanning. Pixels and scans are

spaced 25 km apart at the suborbital point, except the 85-GHz channels are collected at 12.5 km spacing. Every other high-frequency pixel is co-located with the low-frequency pixels, starting with the first pixel in the scan and the first scan in a pair of scans. The channels have resolutions that vary from 12.5x15 km for the 85 GHz (oval due to the slanted viewing angle) to 60x75 km for the 19 GHz.

The polar orbit provides nominal coverage over the latitudes 85°N-S, although limitations in current retrieval techniques prevent useful precipitation estimates in cases of cold land or sea ice.

The SSMI is an operational sensor, so the data record suffers the usual gaps in the record due to processing errors, down time on receivers, etc. Over time the coverage has improved as the operational system has matured. As well, the first 85 GHz sensor to fly degraded quickly due to inadequate solar shielding. After launch in mid-1987, the 85.5 GHz vertical- and horizontal-polarization channels became unusable in 1989 and 1990, respectively. Another issue arose on 14 August 2006: DoD activated the RADCAL beacon on the F15 DMSP, which interfered with the 22V and 85.5V channels, preventing reliable estimates using current GPROF code.

Further details are available in Hollinger et al. (1987, 1990). Note that the acronym was originally "SSM/I", but "SSMI" has since come into common use.

Table 5. The inventory of SSMI data used in the TMPA-RT, period of
record, and sensor status.

DMSP	Period of Record	Status				
F13	29 January 2002 - 18 November 2009	inactive				
F14	29 January 2002 - 23 August 2008	inactive				
F15	29 January 2002 - 14 August 2006	active, but unusable				

.....

The Special Sensor Microwave Imager/Sounder (\*SSMIS\*) is a multi-channel passive microwave radiometer that has flown on selected Defense Meteorological Satellite Program (DMSP) platforms since late 2003. The DMSP is placed in a sun-synchronous polar orbit with a period of about 102 min. The SSMIS provides vertical and horizontal polarization values for the SSMI-like 19, 22, 37, and 91 GHz frequencies (except only vertical at 22) with conical scanning, as well as other channels with a heritage in the Special Sensor Microwave/Temperature 2 (SSM/T2) sensor. Unlike SSMI, every SSMIS scan observes at all channels: pixels and scans are respectively spaced 25 and 12.5 km apart at the suborbital point for channels below 91 GHz, 12.5 km for both pixel and scans for 91 GHz. Thus, the high-frequency channels have twice as many footprints per scan as the lower-frequency channels. Separate feed horns are used for 91 GHz and the rest of the SSMI-like frequencies, so there is not a 1:1 co-location of channel values, as there is for SSMI. The SSMI-like channels have the resolutions

46.5x73.6 km (19, 22 GHz)

31.2x45.0 km (37 GHz)

13.2x15.5 km (91 GHz)

with the slanted viewing angle and in-line processing determining the oval shape.

Operational and design problems early in the program raised serious obstacles to use of the data. Accordingly, the useful periods of record (below) start relatively long after launch. These dates are based on the start of the first publicly available SSMIS as determined by NRL/FNMOC through the Shared Processing Program with NESDIS. In the current version we apply the approximate calibrations developed by D. Vila as part of GPROF2004v (Vila et al. 2013). See "GPROF" for a short summary.

The polar orbit provides nominal coverage over the latitudes 85°N-S, although limitations in current retrieval techniques prevent useful precipitation estimates in cases of cold land or ice.

The SSMIS is an operational sensor, so the data record suffers the usual gaps in the record due to processing errors, down time on receivers, etc. Over time the coverage has improved as the operational system has matured.

Further details are available in Northrup Grumman (2002). Note that the acronym was originally "SSMI/S", but "SSMIS" has since come into common use.

Table 6. The inventory of SSMIS data used in the TMPA-RT, period of record, and sensor status.

DMSP	Period of Record	Status
F16	20 November 2005 - ongoing	active
F17	19 March 2008 - ongoing	active
F18	8 March 2010 - ongoing	active

.....

The Advanced Microwave Sounding Unit B (\*AMSU-B\*) is a multi-channel passive microwave radiometer that flew on selected National Oceanic and Atmospheric Administration (NOAA) platforms from early 2000 to 2011. The NOAA satellites are placed in sun-synchronous polar orbits with periods of about 102 min. The complete AMSU contains 20 channels, the first 15 referred to as AMSU-A, and the last 5 as AMSU-B. These channels (identified as 16 through 20) cover the frequencies 89.0±0.9, 150.0±0.9, and 183.31±1, 3, and 7, all in GHz, with crosstrack scanning. Pixels and scans are spaced 16.3 km apart at nadir, with the pixels increasing in size and changing from circular to elongated in the cross-track direction as one moves away from nadir

The polar orbit provides nominal coverage over the entire globe, although limitations in current retrieval techniques prevent useful precipitation estimates in cases of cold land or sea ice.

The AMSU-B is an operational sensor, so the data record suffers the usual gaps in the record due to processing errors, down time on receivers, etc. Over time the coverage improved as the operational system matured. As well, the NOAA-17 50-GHz channel failed in late October 2003, apparently due to solar flare activity. Finally, NOAA-17 gradually failed during 2010, and eventually it was determined that the Version 7 TMPA-RT should stop using the data at the end of April 2010.

Further details are available in the NOAA KLM User's Guide (September 2000 revision) at

http://www2.ncdc.noaa.gov/docs/klm/index.htm, specifically at

http://www2.ncdc.noaa.gov/docs/klm/html/c3/sec3-4.htm.

Table 7. The inventory of AMSU-B data used in the TMPA, period of record, and sensor status.

Satellite	Period of Record	Status
NOAA-15	1 January 2000 - 14 September 2010	inactive
NOAA-16	4 October 2000 - 16 February 2011	inactive
	(last used for 30 April 2010)	
NOAA-17	28 June 2002 - 17 December 2009	inactive

.....

The Microwave Humidity Sounder (\*MHS\*) is a multi-channel passive microwave radiometer that has flown on selected National Oceanic and Atmospheric Administration (NOAA) platforms since mid-2005 as a follow-on to AMSU-B and on the EUMETSAT MetOp since late 2006. The satellites are placed in sun-synchronous polar orbits with periods of about 102 min. The MHS contains 5 channels, similar to AMSU-B. These channels cover the frequencies 89.0, 157.0, 183.311±1 and 3, and 190.311, all in GHz, with cross-track scanning. Pixels and scans are spaced 16.3 km apart at nadir, with the pixels increasing in size and changing from circular to elongated in the cross-track direction as one moves away from nadir.

The polar orbit provides nominal coverage over the entire globe, although limitations in current retrieval techniques prevent useful precipitation estimates in cases of cold land or sea ice.

The MHS is an operational sensor, so the data record suffers the usual gaps in the record due to processing errors, down time on receivers, etc. Over time the coverage has improved as the operational system has matured.

Further details are available in the NOAA KLM User's Guide (September 2000 revision) at http://www2.ncdc.noaa.gov/docs/klm/index.htm, specifically at http://www2.ncdc.noaa.gov/docs/klm/html/c3/sec3-9.htm.

Table 8. Inventory of MHS data used in the TMPA, period of record, and sensor status.

Satellite	Period of Record	Status
NOAA-18	25 May 2005 – current	active
NOAA-19	9 March 2009 – current	active
MetOp-A	5 December 2006 – current	active
MetOp-B	15 August 2013 – current	active

.....

The infrared (\**IR*\*) data are collected from a variety of sensors flying on the international constellation of geosynchronous-orbit meteorological satellites – the Geosynchronous Operational Environmental Satellites (GOES, United States); the Geosynchronous Meteorological Satellite (GMS, Japan), subsequently Multi-functional Transport Satellite (MTSat, Japan), and then Himawari (Japan); and the Meteorological Satellite (Meteosat,

European Community). There are usually two GOES platforms active covering the eastern and western regions of the Americas, and two Meteoats covering the Europe/Africa and Indian Ocean sectors. The geosynchronous IR data are collected by scanning (parts of) the earth's disk. By international agreement, all satellite operators collect full-disk images at the synoptic observing times (00, 03, ..., 21 UTC) at a minimum.

Subsequent processing is described in "Merged 4-Km IR Tb data set".

The various IR instruments are operational sensors, so the data record suffers the usual gaps in the record due to processing errors, down time on receivers, sensor failures, etc. Most notably during the TMPA-RT period of record, GMS-5 was replaced by GOES-9 starting 01 UTC 22 May 2003, which introduced slightly different instrument characteristics. As well, GMS-5 was replaced by GOES-9 starting 01 UTC 22 May 2003, which introduced slightly different instrument characteristics. Starting 19 UTC 17 November 2005 MTSat-1R went operational, followed by a shift to MTSat-2 on 1 July 2010 and to Himawari 8 at 02 UTC on 7 July 2015.

Further	details	are	available	in	Janowiak	and	Arkin	(1991	).

The inventory of \*sensors contributing to TMPA-RT\* is summarized in Table 9 for convenience; refer to the individual sensor descriptions for additional details.

Table 9. Inventory of sensors contributing to the TPMA-RT data, including start/stop dates, institutional source of the sensor data and precipitation estimate, and explanatory comments.

Sensor	Start Date	End Date	Source	Comment(s)
AMSR-E	19 June 2002	3 Oct 2011	NSIDC AE_Rain.2	frozen at V10/V11
AWISK-E	AWISK-E 19 June 2002		V10 GPROF	(GPROF2004)
SSMI	17 Feb 2000	31 July 2009	CSU GPROF2010	coverage too sparse
DMSP F13	17 Feb 2000		V1a	later
SSMI	17 Feb 2000	22 4 2000	CSU GPROF2010	
DMSP F14	17 Feb 2000	23 Aug 2008	V1a	
SSMI	22 Eab 2000	12 Ana 2006	CSU GPROF2010	RADCAL beacon
DMSP F15	23 Feb 2000	13 Aug 2006	V1a	interference later
SSMIS	20 N 2005	:	CLASS TDR,	start of CLASS TDR
DMSP F16	20 Nov 2005	ongoing	GPROF2004V	archive
SSMIS	10 M 2000	:	CLASS TDR,	start of CLASS TDR
DMSP F17	19 Mar 2008	ongoing	GPROF2004V	archive
SSMIS	9 Man 2010	ongoing	CLASS TDR,	start of CLASS TDR
DMSP F18	8 Mar 2010		GPROF2004V	archive
AMSU-B	17 Eab 2000	14 Can 2010	CICC. CLACC	CICS archive before
NOAA-15	17 Feb 2000	14 Sep 2010	CICS; CLASS	1 June 2007
AMSU-B	4.0-+ 2000	20 4 2010	CICC. CLACC	CICS archive before
NOAA-16	4 Oct 2000	30 Apr 2010	CICS; CLASS	1 June 2007
AMSU-B	20 Ivan 2002	17 Dec 2009	CICC CI ACC	CICS archive before
NOAA-17	28 Jun 2002		CICS; CLASS	1 June 2007
MHS	25 May 2005	ongoing	CICS; CLASS; DDS	CICS archive before

NOAA-18				1 June 2007; DDS after 6 Nov 2012
MHS NOAA-19	9 Mar 2009	ongoing	CICS; CLASS; DDS	CLASS archive starts 7 May 2009; DDS after 6 Nov 2012
MHS MetOp-A	5 Dec 2006	ongoing	CICS; CLASS; DDS	CICS archive before 1 June 2007; DDS after 6 Nov 2012; data gap 14 UTC 27 March 2014–03 UTC 25 May 2014
MHS MetOp-B	15 Aug 2013	ongoing	DDS	
TMI	17 Feb 2000	8 Apr 2015	CSU GPROF2010 V1	
IR	17 Feb 2000	ongoing	CPC 4km Tb	

.....

#### 9. Error Detection and Correction

\*TMI error detection/correction\* is quite similar to that of the SSMI (below) because it is a modified SSMI with the 10 GHz channels added. Built-in hot- and cold-load calibration checks are used to convert counts to antenna temperature (Ta). An algorithm converts Ta to brightness temperature (Tb) for the various channels (eliminating cross-channel leakage). As well, systematic navigation corrections are performed. All pixels with non-physical Tb and local calibration errors are deleted.

Accuracies in the Tb's are within the uncertainties of the precipitation estimation techniques. For the most part, tests show stable cross-calibration with the fleet of SSMI's and SSMIS's.

TRMM is designed to precess over a 46-day period. There is no direct effect on the accuracy of the TMI data, but the continually changing diurnal sampling can cause significant fluctuations in the resulting TMI-only precipitation estimates.

One important test for artifacts is screening the data for "excessive" numbers of "ambiguous pixels"; see that topic for an explanation.

.....

Accuracies in the Tb's are within the uncertainties of the precipitation estimation techniques.

<sup>\*</sup>AMSR-E error detection/correction\* has several parts. Built-in hot- and cold-load calibration checks are used to convert counts to antenna temperature (Ta). An algorithm has been developed to convert Ta to brightness temperature (Tb) for the various channels (eliminating cross-channel leakage). As well, systematic navigation corrections are performed. All pixels with non-physical Tb and local calibration errors are deleted.

One important test for artifacts is screening the data for "excessive" numbers of "ambiguous pixels"; see that topic for an explanation.

.....

\*SSMI error detection/correction\* has several parts. Built-in hot- and cold-load calibration checks are used to convert counts to antenna temperature (Ta). An algorithm has been developed to convert Ta to brightness temperature (Tb) for the various channels (eliminating cross-channel leakage). Differences between the Ta-to-Tb conversions employed by RSS and the U.S. Navy's Fleet Numerical Meteorological and Oceanographic Center imply that uncertainties in the Ta-to-Tb conversion are much larger than any other known uncertainty. Consequently, Colorado State University developed the concept of a Level 1c, which applies corrections developed in the project. In this case, the SSMI Tb's are adjusted to perform as much like the TMI Tb's as possible. As well, systematic navigation corrections are performed. All pixels with non-physical Tb and local calibration errors are deleted.

Accuracies in the Tb's are within the uncertainties of the precipitation estimation techniques. For the most part, tests show only small differences among the SSMI sensors flying on different platforms.

Some satellites experienced significant drifting of the equator-crossing time during their periods of service (see <a href="http://precip.gsfc.nasa.gov/times\_allsat.jpg">http://precip.gsfc.nasa.gov/times\_allsat.jpg</a> for a current time-series plot). There is no direct effect on the accuracy of the SSMI data, but it is possible that the systematic change in sampling time could introduce biases in any resulting SSMI-only precipitation estimates.

One important test for artifacts is screening the data for "excessive" numbers of "ambiguous pixels"; see that topic for an explanation.

.....

\*SSMIS error detection/correction\* has several parts, similar to SSMI. However, Colorado State University is not yet in a position to establish Level 1c datasets, so Ta data sets from NOAA/NCDC are employed in a correction scheme developed by Vila et al. (2013). Errors in the SSMIS Tb's are believed to be "small", except the F16 is known to have some unsolved issues.

In addition, F16 has experienced significant drifting of the equator-crossing time during its period of service (see <a href="http://precip.gsfc.nasa.gov/times\_allsat.jpg">http://precip.gsfc.nasa.gov/times\_allsat.jpg</a> for a current time-series plot). There is no direct effect on the accuracy of the SSMIS data, but it is possible that the systematic change in sampling time could introduce biases in any resulting SSMIS-only precipitation estimates.

One important test for artifacts is screening the data for "excessive" numbers of "ambiguous pixels"; see that topic for an explanation.

.....

\*AMSU-B error detection/correction\* has several parts. Built-in hot- and cold-load calibration checks are used to convert counts to antenna temperature (Ta). Systematic navigation

corrections are performed. All pixels with non-physical Tb and local calibration errors are deleted

Accuracies in the Tb's are within the uncertainties of the precipitation estimation techniques. The main difficulty results from the loss of the NOAA-17 50-GHz channel.

Some satellites experienced significant drifting of the equator-crossing time during their periods of service (see <a href="http://precip.gsfc.nasa.gov/times\_allsat.jpg">http://precip.gsfc.nasa.gov/times\_allsat.jpg</a> for a current time-series plot). There is no direct effect on the accuracy of the AMSU-B data, but it is possible that the systematic change in sampling time could introduce biases in any resulting AMSU-B-only precipitation estimates.

.....

\*MHS error detection/correction\* has several parts. Built-in hot- and cold-load calibration checks are used to convert counts to antenna temperature (Ta). Systematic navigation corrections are performed. All pixels with non-physical Tb and local calibration errors are deleted.

Accuracies in the Tb's are within the uncertainties of the precipitation estimation techniques.

Some of the relevant satellites are beginning to drift in the equator-crossing time during their periods of service (see <a href="http://precip.gsfc.nasa.gov/times\_allsat.jpg">http://precip.gsfc.nasa.gov/times\_allsat.jpg</a> for a current time-series plot). There is no direct effect on the accuracy of the MHS data, but it is possible that the systematic change in sampling time could introduce biases in any resulting MHS-only precipitation estimates.

.....

In common with other microwave algorithms, GPROF flags pixels with certain ranges of Tb values as \*ambiguous pixels\* because such ranges are associated with both real precipitation and artifacts, compared to coincident weather observations. In this approach, the algorithm makes an estimate, but flags it as a possible artifact. GPROF leaves it to the user to evaluate such pixels for use or deletion. Experience shows that if an artifact due to surface effects is responsible, it tends to trigger ambiguous values in the same place repeatedly, and one can capture this by seeing how many of the pixels in the area are flagged. It's a matter of trial and error to set the threshold of "too many" ambiguous pixels to balance dropping good data and including artifacts. In the TMPA-RT the ambiguous pixels are handled as follows:

In the HQ (3B40RT), experience shows that when the fraction of ambiguous (FA) exceeds 40% or the 5x5-grid box average FA exceeds 5%, the precipitation value is likely an artifact. Accordingly, users generally should not employ these values. The likely artifact value is stored as its decremented negative:

$$v = (-100 * p) - 1$$

where p is the floating-point value, v is the scaled-integer value, and v is not equal to the 2-byte-integer missing value (-31999).

This encoding creates a non-physical value that is easy to screen, but preserves the value for subsequent use.

In the calibration for VAR, all flagged precipitation values are accumulated along with the presumably good values. Experience shows that the month-accumulated values should be discarded when accumulated FA exceeds 20%, or the 5x5-grid-box-average accumulated FA exceeds 10%, or the grid box has fewer than 60% of the nominal number of samples for the month at the box's latitude. The resulting holes in the coefficient field are smooth-filled from surrounding grid boxes. In some cases, such as January in Eurasia, these fill-ins can be quite extensive. As a result, our confidence in VAR over wintertime land is reduced. [In the previous, inhomogeneous time series of TMPA-RT data, the full version of this screening was implemented starting with 00Z 2 March 2003. Earlier screens were not consistent and allowed significant artifacts.]

In the combination of HQ and VAR (3B42RT), the HQ values previously judged to be suspect are set to missing before combination with VAR.

.....

The dominant \*IR data correction\* is for slanted paths through the atmosphere. Referred to as "limb darkening correction" in polar-orbit data, or "zenith-angle correction" (Joyce et al. 2001) in geosynchronous-orbit data, this correction accounts for the fact that a slanted path through the atmosphere increases the chances that (cold) cloud sides will be viewed, rather than (warm) surface, and raises the altitude dominating the atmospheric emission signal (almost always lowering the equivalent Tb). The slant path also creates an offset to the geolocation of the IR pixel due to parallax. That is, the elevated cloud top, viewed from an angle, is located closer to the satellite than where the line of sight intersects the Earth's surface. Pixels are moved according to a standard height-Tb-zenith angle profile, at the price of holes created when tall clouds are moved further than shallow clouds behind them. In addition, the various sensors have a variety of sensitivities to the IR spectrum, usually including the 10-11 micron band. Intersatellite calibration differences are documented, but they are not implemented in the current version. They are planned for a future release. The VAR largely corrects inter-satellite calibration, except for small effects at boundaries between satellites. The satellite operators are responsible for detecting and eliminating navigation and telemetry errors.

.....

A number of \*known errors\* are contained in part or all of the current 3B42RT archive. They have been uncovered by visual inspection and other diagnostics, but correction awaits the next retrospective processing. Other items will be included in future re-processing cycles as possible. For ease of document maintenance, some of the following items imply the known error by stating what upgrade was applied.

1. AMSU-B and MHS estimates are deficient in sensing light precipitation, leading to an underestimate that is regionally dependent, but can approach 100% in light-rain areas. Because of this, the AMSU-B estimates are used only if no other HQ estimates are available, meaning that the deficiency is minimized in the TMPA-RT. Nonetheless, it causes bias over

- oceans that begins in 2000 and fluctuates with the coverage by AMSU-B and MHS estimates.
- 2. GPROF estimates have a variety of artifacts associated with coastal regions that are sensorand scene-dependent. In particular, inland water bodies in the Southeastern U.S. (Tian and Peters-Lidard 2007), Lake Nasar in Egypt, and desert coastal regions show anomalous high precipitation, while oceanic coastal regions in a variety of rainy situations tend to be deficient in precipitation.
- 3. SSMIS calibration and updates to the GPROF-SSMIS algorithm continue. The present solution for these issues is considered satisfactory, but not definitive.
- 4. The TMPA-RT data cut-off has been set at about 8 hours after observation time. At least occasionally with SSMIS, and more frequently with MHS, the input data arrive too late to be included in the HQ (3B40RT) run for that hour.
- 5. The current satellite-gauge combination scheme allows coastal gauge data to "bleed" into coastal waters, up to 1° away from the coast. This is particularly noticeable where there is heavy precipitation in the gauge analysis, but modest values off-shore.

.....

Some \*known anomalies\* in the data set are documented and left intact at the discretion of the data producers. As a real-time system the TMPA-RT has gaps due to delays in data delivery. Generally, no attempt is made to process data that arrives after the cut-off time. These gaps largely disappear as the Version 7 TRMM product 3B42 is computed (see"3B42").

- 1. The TRMM orbital altitude was raised from 350 to 401.5 km in August 2001 to extend the life of the mission by reducing the amount of fuel needed to maintain the orbit. This caused small changes in footprint size and minimum detectable precipitation rates. The Version 7 algorithms are supposed to account for these changes, but tests show small unavoidable differences that are still being researched.
- 2. The TRMM PR suffered an electronics failure on 29 May 2009. Data were lost until the "B-side" electronics were activated on 19 June 2009. Small residual differences remain between A-side and B-side data.
- 3. At 2045 UTC on 21 March 2012 GOES-15 (WEST) suffered a "bad momentum unload" and ceased recording data. Imaging was restored at 1722 UTC on 23 March 2012. In the interim GOES-13 (EAST) was shifted to recording full-disk images. Use of higher-zenith-angle GOES-13 and MTSat-1 data largely covers the gap caused by the GOES-15 drop-outs.
- 4. The mix of satellites has changed over time, which affects the overall performance of the algorithm in two ways. First, the relative weighting of conically scanning microwave imagers versus cross-track-scanning sounders shifts, and second, the relative proportion of IR-based estimates changes. The passive-microwave sensor inventory is shown in "sensors contributing to TMPA-RT".
- 5. The V7 3B43 tropical-ocean average precipitation is consistently some 5% higher than the combined TMI-PR product (2B31) that serves as the calibrator (see "intercomparison results"). The basis for this difference is not explicated at this point, but the value is small enough and consistent enough that we chose to release the data as background work continues.

- 6. Occasional IR datasets were discovered to be corrupted in the retrospective processing; these were simply skipped, since each hour of IR data is composed of data from the current and previous half-hour fields.
- 7. F17 SSMIS has anomalously high precip values for a few scans over Brazil in the 21Z 26 April 2013 3B42 HQ and multi-satellite precip fields.
- 8. A TRMM spacecraft anomaly resulted in the loss of most TRMM sensor data for the period 02-14 UTC on 12 November 2013, and additional issues resulted in data gaps during the period 2000-2330 UTC. This reduces the data content in 3B40RT and 3B42RT somewhat, but is not a serious issue overall.
- 9. Snow accumulation on the receiving antenna prevented reception of MTSAT-2 data from 1832 UTC on 14 February 2014 to 1232 UTC on 15 February 2014. The data are lost.
- 10. Metop-A experienced an anomaly that prevented data collection for 1400 UTC 27 March 2014–0746 UTC 21 May 2014. Data were re-introduced to TMPA-RT beginning with 03 UTC 25 May 2014.

Several exceptions have been made to the no-reprocessing rule:

1. As described in "additional processing for Version 7", the entire retrospective processing was re-done to pick up AMSU and MHS data that had been accidentally ignored, and to correctly put "missing" values where they belonged in 3B42RT.

.....

## 10. Missing Value Estimation and Codes

There is generally no effort to \*estimate missing values\* in the single-source input data sets.

.....

All products in the TMPA-RT use the \*standard missing value\* "-31999". In addition, grid boxes suspected of having artifacts and all non-missing values in grid boxes outside the latitude band 50°N-S are considered to be highly uncertain, and are encoded to negative values. Accordingly, users generally should not employ these values.

.....

All \*missing hours\* of a product result from completely absent input data for the given hour. If the input file(s) is(are) available, the product file is created, even if it lacks any valid data.

.....

# 11. Quality and Confidence Estimates

The \*accuracy\* of the precipitation products can be broken into systematic departures from the true answer (bias) and random fluctuations about the true answer (sampling), as discussed in Huffman (1997). The former are the biggest problem for climatological averages, since they will not average out. However, for short averaging periods the low number of samples and/or algorithmic inaccuracies tend to present a more serious problem for individual microwave data sets. That is, the sampling is spotty enough that the collection of values over, say, one day may not be representative of the true distribution of precipitation over the day. For VAR, the

sampling is good, but the algorithm likely has substantial RMS error due to the weak physical connection between IR Tb's and precipitation.

Accordingly, the "random error" is assumed to be dominant, and estimates could be computed as discussed in Huffman (1997). Random error cannot be corrected.

The "bias error" is likely small, or at least contained. This is less true over land, where the lower-frequency microwave channels are not useful for precipitation estimation with our current state of knowledge. The state of the art at the monthly scale is reflected in the study by Smith et al. (2006) and Adler et al. (2012). One study of the sub-monthly bias is provided by Tian et al. (2009).

.....

The TMPA-RT \*intercomparison results\* continue to be developed. The time series of the global images shows good continuity in time and space across the geo-IR data boundaries. Overall, the analysis approach appears to be working as expected. See Huffman et al. (2007, 2010) for more information. Numerous studies by the community are listed in the summary of citations:

ftp://meso-a.gsfc.nasa.gov/pub/trmmdocs/rt/TMPA\_citations.pdf.

Validation studies are being conducted under the auspices of the International Precipitation Working Group (IPWG) in Australia, the continental U.S., western Europe, parts of South America, and Japan (Ebert et al. 2007). Respectively, the web sites for these activities are:

http://cawcr.gov.au/projects/SatRainVal/validation-intercomparison.html

http://cics.umd.edu/~johnj/us web.html

http://meso-a.gsfc.nasa.gov/ipwg/ipwgeu\_home.html

http://cics.umd.edu/~dvila/web/SatRainVal/dailvval.html

http://www-ipwg.kugi.kyoto-u.ac.jp/IPWG/sat val Japan.html

Zhou et al. (2014) provide a creative "double mass" analysis showing how the time series of 3B42 and 3B42RT differ by location. It is possible that an extension of this approach would illuminate the changes introduced by the climatological calibration in October 2014.

.....

The \*diurnal cycle\* depicted in the 3-hourly 3B42RT V7 (and all other versions) is affected by the particular mix of satellite sensors at any given time and place, in common with all other such satellite-based precipitation estimation systems. The diurnal cycle phase produced by IR estimates, which respond to cloud tops, is known to lag the phase of surface observations in many locations. The lag is highly variable, but frequently reported as up to 3 hours. The passive microwave estimates over land depend on the solid hydrometeors, which typically are confined to the upper reaches of clouds. This dependence also leads to lags compared to surface observations, up to about 1.5 hours. Over ocean the passive microwave estimates are driven by the full vertical profile of precipitation for imagers, but primarily by solid hydrometeors for sounders. Thus, there is a mix of typical lags, minimal for imagers and up to 1.5 hours for sounders. When you consider the regional variability in the lags of the individual sensor types and the variable mix of sensors contributing to the diurnal cycle during different epochs of

satellite coverage, the general statement is that lags are more likely early in the dataset, before many passive microwave satellites were available, and are more likely over land. The TRMM PR, being a radar, gives relatively unbiased estimates of the diurnal cycle, but its sampling is so sparse that it takes several years of data to allow a reasonable estimate to appear out of the sampling noise. See Kikuchi and Wang (2008), although their study with Version 6 will have larger lags due to concentrating early in the record and with fewer passive microwave satellites than Version 7 has for the bulk of their study period.

.....

The \*controlling factors on dataset performance\* critically depend on the calibration approach, since the time series of the completed data tend to follow the time series of the calibrator, at least on the large scale. All of the global precipitation data sets have some calibrating data source, which is necessary to control bias differences between contributing satellites. Otherwise, shifts in the contributing set of satellites at any given time can cause unphysical shifts in the behavior of the precipitation estimates. However, this calibration plays a large role in determining the interannual variation that the various data sets display. Experience shows that datasets/regions with passive microwave calibration (oceans for Global Precipitation Climatology Project [GPCP] monthly Satellite-Gauge [SG], and all regions for 3B42RT and the Integrated Multi-satellitE Retrievals for Global Precipitation Measurement [GPM] mission [IMERG] Early and Late) tend to have similar interannual fluctuations, while datasets/regions with combined passive/active microwave calibration (oceans for 3B42/43 and IMERG Final) tend to show a variation in the tropical oceans that leads the passive microwave-calibrated datasets by 3-6 months. Climatological calibrations might change the mean bias or even the seasonal cycle, but they should not change the interannual variations or long-term trends.

Analyses of monthly surface gauge data add another layer of calibration over land in some datasets. The combined precipitation research team at Goddard has major responsibility for the GPCP monthly SG combined product, the 3B43 monthly product, and the IMERG Final Run monthly product. In each case the multi-satellite data are averaged to the monthly scale and combined with the Global Precipitation Climatology Centre's (GPCC) monthly surface precipitation gauge analysis. In each case the multi-satellite data are adjusted to the large-area mean of the gauge analysis, where available (mostly over land), and then combined with the gauge analysis using a simple inverse estimated-random-error variance weighting. In all three data sets the gauge analysis has an important or dominant role in determining the final combined value for grid boxes in areas with "good" gauge coverage. [See Bolvin et al. (2009) for an example with GPCP.] Regions with poor gauge coverage, such as central Africa have a higher weight on the satellite input that has been corrected to the large-area bias of the gauges. The oceans are mostly devoid of gauges and therefore mostly lack such gauge input.

In contrast, the short-interval (as opposed to monthly, above) GPCP is the One-Degree Daily (1DD), the short-interval TMPA is 3B42 (3-hourly), and the short-interval IMERG (half-hourly). In each case the short-interval data are adjusted with a simple, spatially varying ratio to force the multi-satellite estimates to approximately average up to the corresponding monthly satellite-gauge product, with controls on the ratios to prevent unphysical results. Thus, monthly-average values of the short-interval data should be close to the average of the monthly datasets, which the developers consider more reliable than the short-interval datasets. In fact, compared to datasets

that lack the adjustment to the monthly satellite-gauge estimates, the 1DD, 3B42, and IMERG Final half-hourly datasets tend to score better at timescales longer than a few days. This is presumably because the random error begins to cancel out as more samples are averaged together, leaving only the bias error. Of course, the short-interval datasets and regions that lack month-to-month surface gauge data input are more clearly driven by the behavior of the satellite input data.

.....

#### 12. Data Archives

The \*archive and distribution site\* for the official release of the TRMM Real-Time Multi-Satellite Precipitation Analysis is:

Helpdesk Precipitation Processing System Code 610.2 NASA Goddard Space Flight Center Greenbelt, MD 20771 USA

Phone: 301-614-5184 Fax: 301-614-5575

Internet: helpdesk@pps-mail.nascom.nasa.gov
Anonymous FTP: ftp://trmmopen.gsfc.nasa.gov/pub/merged

Interactive Web-based access to the data and related fields is provided through Giovanni; see that topic for details.

Independent archive and distribution sites exist for the input data sets, and contact information may be obtained through G.J. Huffman (see "Documentation creator").

.....

\*DOIs for 3B40RT, 3B41RT, and 3B42RT\* have been assigned using GPM-style naming. For completeness, this list also includes the TMP products and two value-added products computed at the GDISC that give daily accumulations.

Local file ID	DOI
TRMM_3B40RT_7	10.5067/TRMM/TMPA/3H-E-MW/7
TRMM_3B41RT_7	10.5067/TRMM/TMPA/3H-E-IR/7
TRMM_3B42RT_7	10.5067/TRMM/TMPA/3H-E/7
TRMM_3B42_7	10.5067/TRMM/TMPA/3H/7
TRMM_3B43_7	10.5067/TRMM/TMPA/MONTH/7
TRMM_3B42_Daily_7	10.5067/TRMM/TMPA/DAY/7
TRMM_3B42RT_Daily_7	10.5067/TRMM/TMPA/DAY-E/7

The full URL is https://doi.org/<DOI>.

.....

#### 13. Documentation

The \*documentation creator\* is:

Dr. George J. Huffman Code 612 NASA Goddard Space Flight Center Greenbelt, MD 20771 USA

Phone: +1-301-614-6308 Fax: +1-301-614-5492

Internet: george.j.huffman@nasa.gov MAPL Precipitation Page: http://precip.gsfc.nasa.gov/

.....

## The \*documentation revision history\* is:

```
14 February 2002
                    Draft 1
                               by GJH
21 February 2002
                               by GJH
                    Version 1
22 March 2002
                    Rev. 1.1
                               by GJH
02 March 2003
                    Rev. 1.2
                               by GJH
25 September 2003
                    Rev. 1.3
                               by GJH
                               by GJH
23 February 2003
                    Rev. 1.4
10 October 2003
                    Rev. 1.5
                               by GJH
15 April 2004
                    Rev. 1.6
                               by GJH
23 November 2004
                    Rev. 1.7
                               by GJH,EJN
                               by GJH,EJN,DTB
16 December 2004
                    Rev. 1.8
23 December 2004
                    Rev. 1.9
                               By GJH
03 February 2005
                    Rev. 1.10
                               by GJH
10 March 2005
                    Rev. 1.11
                               by GJH
27 September 2005
                    Rev. 1.12
                               by GJH
05 June 2006
                    Rev. 1.13
                               by GJH
08 September 2006
                    Rev. 1.14
                              by GJH
12 September 2006
                    Rev. 1.15
                               by GJH
21 September 2006
                    Rev. 1.16
                               by GJH
06 April 2006
                    Rev. 1.17
                               by GJH
03 October 2007
                    Rev. 1.18
                               by GJH
30 October 2007
                    Version 2
                               by GJH,EJN,DTB – MSWord and PDF
28 December 2008
                    Rev. 2.2
                               by GJH
1 May 2008
                    Rev. 2.3
                               by GJH
                    Rev. 2.4
17 February 2009
                               by GJH, EJN, DTB
12 March 2009
                    Rev. 2.5
                               by GJH
13 May 2009
                    Rev. 2.6
                               by GJH
08 September 2009
                    Rev. 2.7
                               by GJH
12 November 2009
                    Rev. 2.8
                               by GJH
18 November 2009
                    Rev. 2.9
                               by GJH
14 December 2009
                    Rev. 2.10
                               by GJH
```

```
17 February 2010
                    Rev. 2.11
                               by GJH
16 November 2010
                    Rev. 2.12
                              by GJH
6 January 2010
                    Rev. 2.13
                              by GJH
16 February 2011
                    Rev. 2.14
                              by GJH
14 April 2011
                    Rev. 2.15
                               by GJH
6 May 2011
                    Rev. 2.16
                              by GJH
31 May 2011
                    Rev. 2.17
                               by GJH
14 March 2012
                    Rev. 2.18
                               by GJH
25 June 2012
                    Version 3
                              by GJH
25 September 2012
                    Rev. 3.2
                               by GJH
                    Rev. 3.3
28 January 2013
                               by GJH
                               by GJH
16 August 2013
                    Rev. 3.4
15 February 2014
                    Rev. 3.5
                               by GJH
25 May 2014
                    Rev. 3.6
                               by GJH
9 April 2015
                               by GJH; end of mission content
                    Rev. 2.7
7 July 2015
                    Rev. 2.7
                               by DTB,GJH; R code reader, Himawari 8
19 April 2017
                    Rev. 2.8
                               by GJH; update IMERG, Giovanni comments
                               by GJH; 2A12 thresholding
28 June 2017
                    Rev. 2.9
                              by GJH; DOIs; IMERG timing
26 April 2018
                    Rev. 2.10
```

.....

The list of \*references\* used in this documentation is:

- Adler, R.F., G. Gu, G.J. Huffman, 2012: Estimating Climatological Bias Errors for the Global Precipitation Climatology Project (GPCP). *J. Appl. Meteor. and Climatol.*, **51**(1), doi:10.1175/JAMC-D-11-052.1, 84-99.
- Andersson, A., K. Fennig, C. Klepp, S. Bakan, H. Graßl, J. Schulz, 2010: The Hamburg Ocean Atmosphere Parameters and Fluxes from Satellite Data HOAPS-3. *Earth Syst. Sci. Data*, **2**, 215-234, doi:10.5194/essd-2-215-2010.
- Bolvin, D.T., R.F. Adler, G.J. Huffman, E.J. Nelkin, J.P. Poutiainen, 2009: Comparison of GPCP Monthly and Daily Precipitation Estimates with High-Latitude Gauge Observations. *J. Appl. Meteor. Climatol.*, **48**, 1843–1857.
- Chiu, L.S., R. Chokngamwong, 2010: Microwave Emission Brightness Temperature Histograms (METH) Rain Rates for Climate Studies: Remote Sensing Systems SSM/I Version-6 Results. *J.Appl. Met. Clim.*, **49**, 115-123.
- Grody, N.C., 1991: Classification of snow cover and precipitation using the Special Sensor Microwave/Imager (SSM/I). *J. Geophys. Res.*, **96**, 7423-7435.
- Haddad, Z.S., D.A. Short, S.L. Durden, E. Im, S. Hensley, M.B. Grable, R.A. Black, 1997a: A New Parameterization of the Rain Drop Size Distribution. *IEEE Trans. Geosci. Remote Sens.*, **35**, 532-539.
- Haddad, Z.S., E.A. Smith, C.D. Kummerow, T. Iguchi, M.R. Farrar, S.L. Durden, M. Alves, W.S. Olson, 1997b: The TRMM "Day-1" Radar/Radiometer Combined Rain-Profiling Algorithm. *J. Meteor. Soc. Japan*, **75**, 799-809.
- Hollinger, J., R. Lo, G. Poe, J. Pierce, 1987: Special Sensor Microwave/Imager User's Guide, Naval Res. Lab., Washington, DC.

- Hollinger, J.P., J.L. Pierce, G.A. Poe, 1990: SSM/I instrument evaluation. *IEEE Trans. Geosci. Remote Sens.*, **28**, 781-790.
- Huffman, G.J., 1997: Estimates of root-mean-square random error contained in finite sets of estimated precipitation. *J. Appl. Meteor.*, **36**, 1191-1201.
- Huffman, G.J., R.F. Adler, D.T. Bolvin, G. Gu, E.J. Nelkin, K.P. Bowman, Y. Hong, E.F. Stocker, D.B. Wolff, 2007: The TRMM Multi-satellite Precipitation Analysis: Quasi-global, multi-year, combined-sensor precipitation estimates at fine scale. *J. Hydrometeor.*, **8**(1), 38-55. PDF available at ftp://meso.gsfc.nasa.gov/agnes/huffman/papers/TMPA jhm 07.pdf.gz
- Huffman, G.J., R.F. Adler, D.T. Bolvin, E.J. Nelkin, 2010: The TRMM Multi-satellite Precipitation Analysis (TMPA). Chapter 1 in *Satellite Applications for Surface Hydrology*, F. Hossain and M. Gebremichael, Eds. Springer Verlag, ISBN: 978-90-481-2914-0, 3-22. PDF available at *ftp://meso.gsfc.nasa.gov/agnes/huffman/papers/TMPA hydro rev.pdf*
- Huffman, G.J., R.F. Adler, S. Curtis, D.T. Bolvin, E.J. Nelkin, 2007: Global rainfall analyses at monthly and 3-hr time scales. Chapter 23 of *Measuring Precipitation from Space: EURAINSAT and the Future*, V. Levizzani, P. Bauer, and F.J. Turk, Eds., Springer Verlag (Kluwer Academic Pub. B.V.), Dordrecht, The Netherlands, 291-306. [Invited paper]
- Huffman, G.J., R.F. Adler, E.F. Stocker, D.T. Bolvin, E.J. Nelkin, 2003: Analysis of TRMM 3-hourly multi-satellite precipitation estimates computed in both real and post-real time. *Combined Preprints CD-ROM*, 83rd AMS Annual Meeting. Paper P4.11 in 12th Conf. on Sat. Meteor. and Oceanog., 9-13 Feb. 2003, Long Beach, CA, 6 pp.
- Huffman, G.J., D.T. Bolvin, D. Braithwaite, K. Hsu, R. Joyce, C. Kidd, E.J. Nelkin, S. Sorooshian, J. Tan, P. Xie, 2018: Algorithm Theoretical Basis Document (ATBD) Version 5.2 for the NASA Global Precipitation Measurement (GPM) Integrated Multi-satellitE Retrievals for GPM (I-MERG). GPM Project, Greenbelt, MD, 35 pp. <a href="https://pmm.nasa.gov/sites/default/files/document\_files/IMERG\_ATBD\_V5.2.pdf">https://pmm.nasa.gov/sites/default/files/document\_files/IMERG\_ATBD\_V5.2.pdf</a>
- Janowiak, J.E., P.A. Arkin, 1991: Rainfall variations in the tropics during 1986-1989. *J. Geophys. Res.*, **96**, 3359-3373.
- Jost, V., S. Bakan, K. Fennig, 2002: HOAPS A new satellite-derived freshwater flux climatology. *Meteorol. Zeit.*, **11**, 61-70.
- Joyce, R.J., J.E. Janowiak, P.A. Arkin, P. Xie, 2004: CMORPH: A method that produces global precipitation estimates from passive microwave and infrared data at 8 km, hourly resolution. *J. Climate*, **5**, 487-503.
- Joyce, R.J., J.E. Janowiak, G.J. Huffman, 2001: Latitudinal and seasonal dependent zenith angle corrections for geostationary satellite IR brightness temperatures. *J. Appl. Meteor.*, **40**(4), 689-703.
- Kikuchi, K., B. Wang, 2008: Diurnal Precipitation Regimes in the Global Tropics. *J. Climate*, **21**, doi:10.1175/2007JCLI2051.1, 2680-2696.
- Kongoli, C., P. Pellegrino, R. Ferraro, 2007: The utilization of the AMSU high frequency measurements for improved coastal rain retrievals. *Geophys. Res. Lett.*, **34**, L17809, doi:10.1029/2007GL029940.
- Kubota T., S. Shige, H. Hashizume, K. Aonashi, N. Takahashi, S. Seto, M. Hirose, Y.N. Takayabu, K. Nakagawa, K. Iwanami, T. Ushio, M. Kachi, K. Okamoto, 2007: Global precipitation map using satellite-borne microwave radiometers by the GSMaP Project: Production and validation. *IEEE Trans. Geosci. Remote Sens.* 45, 2259-2275.

- Kummerow, C., W.S. Olson, L. Giglio, 1996: A simplified scheme for obtaining precipitation and vertical hydrometeor profiles from passive microwave sensors. *IEEE Trans. Geosci. Remote Sens.*, **34**, 1213-1232.
- Kummerow, C., W. Barnes, T. Kozu, J. Shiue, J. Simpson, 1998: The Tropical Rainfall Measuring Mission (TRMM) sensor package. *J. Atmos. Oceanic Tech.*, **15**(3), 809-817.
- Northrup Grumman, 2002: Algorithm and Data User Manual (ADUM) for the Special Sensor Microwave Imager/Sounder (SSMIS). Northrup Grumman Electronic Systems, Azusa, CA, Report 12621, 69 pp. ftp://rain.atmos.colostate.edu/pub/msapiano/SSMI\_SSMIS\_Archive\_Docs/SSMIS general/Algorithm and Data User Manual For SSMIS Jul02.pdf
- Parsons, M.A., R. Duerr, J.-B. Minster, 2010: Data Citation and Peer Review. EOS, 91(34), 297-298.
- PMM, 2014: Goodbye to TRMM, First Rain Radar in Space. http://pmm.gsfc.nasa.gov/articles/goodbye-trmm-first-rain-radar-space.
- Smith, T.M., P.A. Arkin, J.J. Bates, G.J. Huffman, 2006: Estimating bias of satellite-based precipitation estimates. *J. Hydrometeor.*, 7(5), 841-856.
- Sorooshian, S., K.-L. Hsu, X. Gao, H.V. Gupta, B. Imam, D. Braithwaite 2000: Evaluation of PERSIANN system satellite-based estimates of tropical rainfall. *Bull. Amer. Meteor. Soc.*, **81**, 2035-2046.
- Spencer, R.W., 1993: Global oceanic precipitation from the MSU during 1979-92 and comparisons to other climatologies. *J. Climate*, **6**, 1301-1326.
- Tian, Y., C.D. Peters-Lidard, 2007: Systematic anomalies over inland water bodies in satellite-based precipitation estimates. *Geophys. Res. Lett.*, **34**, doi:1029/2007GL030787.
- Tian, Y., C. Peters-Lidard, J. Eylander, R. Joyce, G. Huffman, R. Adler, K.-L. Hsu, F. J. Turk, M. Garcia, J. Zeng, 2009: Component Analysis of Errors in Satellite-Based Precipitation Estimates. *J. Geophys. Res. Atmos.*, **114**, D22104, doi:10.1029/2009JD011949.
- Turk, F.J., G.D. Rohaly, J. Hawkins, E.A. Smith, F.S. Marzano, A. Mugnai, V. Levizzani, 1999: Meteorological applications of precipitation estimation from combined SSM/I, TRMM and infrared geostationary satellite data. *Microwave Radiometry and Remote Sensing of the Earth's Surface and Atmosphere*, P. Pampaloni and S. Paloscia Eds., VSP Int. Sci. Publ., 353-363.
- Vila, D., R. Ferraro, R. Joyce, 2007: Evaluation and improvement of AMSU precipitation retrievals. *J. Geophys. Res.*, **112**, D20119, doi:10.1029/2007JD008617.
- Vila, D., C. Hernandez, R. Ferraro, H. Semunegus, 2013: The Performance of Hydrological Monthly Products Using SSM/I SSMI/S Sensors. *J. Hydrometeor.*, **14**, doi:10.1175/JHM-D-12-056.1, 266-274.
- Villarini, G., W.F. Krajewski, 2007: Evaluation of the research-version TMPA three-hourly 0.25°x0.25° rainfall estimates over Oklahoma. *Geopys. Res. Lett.*, **34**, doi:10.1029/2006GL029147.
- Weng, F., L. Zhao, R. Ferraro, G. Poe, X. Li, N. Grody, 2003: Advanced Microwave Sounding Unit cloud and precipitation algorithms. *Radio Sci.*, **38**, 8068-8079.
- Wentz, F.J., and R.W. Spencer, 1998: SSM/I rain retrievals within a unified all-weather ocean algorithm. *J. Atmos. Sci.*, **55**(9), 1613-1627.
- Wilheit, T., A. Chang, L. Chiu, 1991: Retrieval of Monthly Rainfall Indices from Microwave Radiometric Measurements Using Probability Distribution Function. *J. Atmos. Ocean. Tech.*, **8**, 118-136.
- Yong, B., B. Chen, Y. Hong, J.J. Gourley, Z. Li, 2015: Impact of Missing Passive Microwave Sensors on Multi-Satellite Precipitation Retrieval Algorithm. *Rem. Sens.*, in review.

Zhao, L., F. Weng, 2002: Retrieval of ice cloud parameters using the Advanced Microwave Sounding Unit. *J. Appl. Meteor.*, **41**, 384-395.

Zhou, T., B. Nijssen, G.J. Huffman, D.P. Lettenmaier, 2014: Evaluation of the TRMM Real-Time Multi-Satellite Precipitation Analysis Version 7 for Macroscale Hydrologic Prediction. *J. Hydrometeor.*, **15**(4), 1651–1660. *doi: http://dx.doi.org/10.1175/JHM-D-13-0128.1*.

#### Web Sites:

AMS data citation policy: http://www2.ametsoc.org/ams/index.cfm/publications/authors/journal-and-bams-authors/journal-and-bams-authors-guide/data-archiving-and-citation/AMSR instrument: http://www.ghcc.msfc.nasa.gov/AMSR/

AMSU-B instrument: http://www2.ncdc.noaa.gov/docs/klm/html/c3/sec3-4.htm in the NOAA KLM User's Guide (September 2000 revision):

http://www2.ncdc.noaa.gov/docs/klm/index.htm

Giovanni: https://giovanni.sci.gsfc.nasa.gov/giovanni/

IMERG ATBD: https://pmm.nasa.gov/sites/default/files/document\_files/IMERG\_ATBD\_V5.2.pdf IPWG Validation for Australia: http://cawcr.gov.au/projects/SatRainVal/validation-intercomparison.html

IPWG Validation for U.S.: http://cics.umd.edu/~johnj/us web.html

IPWG Validation for western Europe: http://meso-a.gsfc.nasa.gov/ipwg/ipwgeu\_home.html

IPWG Validation for South America: http://cics.umd.edu/~dvila/web/SatRainVal/dailyval.html

IPWG Validation for Japan: http://www-ipwg.kugi.kyoto-u.ac.jp/IPWG/sat\_val\_Japan.html

MAPB Precipitation Page: http://precip.gsfc.nasa.gov/

MHS instrument: http://www2.ncdc.noaa.gov/docs/klm/html/c3/sec3-9.htm in the NOAA KLM User's Guide (September 2000 revision):

http://www2.ncdc.noaa.gov/docs/klm/index.htm

PPS home: http://pps.gsfc.nasa.gov

Satellite overpass times: http://precip.gsfc.nasa.gov/times\_allsat.jpg

TMPA data: http://trmm.gsfc.nasa.gov/data\_dir/data.html

TMPA and TMPA-RT citations:

ftp://meso-a.gsfc.nasa.gov/pub/trmmdocs/rt/TMPA citations.pdf

TMPA-RT Data: ftp://trmmopen.gsfc.nasa.gov/pub/merged/

TMPA-RT paper: ftp://meso.gsfc.nasa.gov/agnes/huffman/papers/TMPA\_jhm\_07.pdf.gz TMPA-RT update: ftp://meso.gsfc.nasa.gov/agnes/huffman/papers/TMPA\_hydro\_rev.pdf

TRMM home: http://trmm.gsfc.nasa.gov/

.....

## \*Acronyms\*

ASCII American Standard Code for Information Interchange (i.e., text)

AIRS Atmospheric Infrared Sounder

AMSR-E Advanced Microwave Scanning Radiometer for Earth Observing System

AMSU Advanced Microwave Sounding Unit
ATBD Algorithm Theoretical Basis Document
AVHRR Advanced Very High Resolution Radiometer

CMORPH CPC MORPHing algorithm

CMORPH-KF Kalman Filter version of CMORPH

CPC Climate Prediction Center

CPU Central Processing Unit (of a computer)

De particle effective diameter size

DMSP Defense Meteorological Satellite Program

DOI Digital Object Identifier

EUMETSAT EUropean organization for the exploitation of Meteorological Satellites

FA Fraction of Ambiguous

FNMOC Fleet Numerical Meteorological and Oceanographic Center

FTP File Transfer Protocol

GDAS Global Data Assimilation System

GHz Gigahertz

GMS Geosynchronous Meteorological Satellite

GOES Geosynchronous Operational Environmental Satellites

GPM Global Precipitation Measurement mission

GPROF Goddard Profiling algorithm
GSFC Goddard Space Flight Center

GSMaP Global Satellite Map of Precipitation HQ High Quality (microwave precipitation)

IDL Interactive Data Language

IMERG Integrated Multi-satellitE Retrievals for GPM INTEGRATION IN

IR Infrared

IWP Ice Water Path

JAXA Japanese Aerospace Exploration Agency

KB Kilobytes

lat/lon latitude/longitude LEO Low Earth orbit

MAPL Mesoscale Atmospheric Processes Laboratory

MB megabytes

Meteorological Satellite

MetOp Operational Meteorological satellite
MHS Microwave Humidity Sounder

MM5 NCAR/PSU Mesoscale Model Version 5

MSPPS Microwave Surface and Precipitation Products System

MSU Microwave Sounding Unit

MTSat Multifunctional Transport Satellite

NASA National Aeronautics and Space Administration NCAR National Center for Atmospheric Research

NCDC National Climatic Data Center

NESDIS National Environmental Satellite Data and Information Service

NOAA National Oceanic and Atmospheric Administration

NWS National Weather Service

PERSIANN Precipitation Estimation from Remotely Sensed Information using Artificial

Neural Networks

PERSIANN-CCS

PERSIANN with Cloud Classification System

PPS Precipitation Processing System PSU Pennsylvania State University

RT Real Time

SDR Satellite Data Record

SSMI Special Sensor Microwave/Imager

SSMIS Special Sensor Microwave Imager-Sounder SSM/T2 Special Sensor Microwave/Temperature 2

Ta Antenna Temperature
Tb Brightness Temperature

TCI TRMM Combined Instrument algorithm (2B31)

TMI TRMM Microwave Imager

TMPA TRMM Multi-satellite Precipitation Algorithm

TMPA-RT Real-Time TMPA

TRMM Tropical Rainfall Measuring Mission

URL Universal Resource Location

UTC Universal Coordinated Time (same as GMT, Z)

VAR VAriable Rainrate (IR precipitation)

V6 Version 6 V7 Version 7

.....

#### 14. Inventories

The \*data set inventory\* may be obtained by accessing the anonymous FTP site at PPS ftp://trmmopen.gsfc.nasa.gov/pub/merged/ or contacting the representative listed in section 12.

.....

### 15. How to Order Data and Obtain Information about the Data

Users interested in \*obtaining data\* should access the anonymous FTP site at PPS ftp://trmmopen.gsfc.nasa.gov/pub/merged/ or contact the representative listed in Section 12.

As well, Web-based interactive access to the TMPA-RT and related data is provided by Giovanni; see that topic for details.

.....

The \*data access policy\* is "freely available" with three common-sense caveats:

1. It is an emerging best practice that the data set source should be referenced when the data are used. Current TMPA data sets have not been given DOI's. A formal reference of the form

Huffman, G.J., E.F. Stocker, D.T. Bolvin, E.J. Nelkin, 2014, last updated 2014: <*dataset identifier> Data Sets.* NASA/GSFC, Greenbelt, MD, USA, <dataset archive *URL>*.

where <dataset archive URL> is now given by the DOI (see "DOIs for 3B40RT, 3B41RT, and 3B42RT"), is suggested following the AMS policy statement at

http://www2.ametsoc.org/ams/index.cfm/publications/authors/journal-and-bams-authors/journal-and-bams-authors-guide/data-archiving-and-citation/.

Note that the AMS policy states that this dataset reference should be in addition to reference to the relevant papers on constructing the data set. This approach allows readers to find both the technical literature and the data archive.

- 2. New users should obtain their own current, clean copy, rather than taking a version from a third party that might be damaged or out of date.
- 3. Errors and difficulties in the dataset should be reported to the dataset creators.

.....

# 16. Appendices

# Appendix 16.1 \*Read a File of Data, C Example\*

A file of data may be read with many standard data-display tools. The 2880-byte header is designed to be exactly the size of one row of data, so the header may be bypassed by skipping 2880 bytes or 1440 2-byte integer data points or one row. Alternatively, the data may be output under program control as demonstrated in this C example. Once past the header, there are always a precipitation field, a random error field, and 1-5 auxiliary fields. As documented in "Data File Layout", the grids are either 1440x720 (3B40RT) or 1440x480 (3B41RT, 3B42RT) and the data are either scaled 2-byte integer (precipitation, random error, and uncalibrated precipitation) or 1-byte integer (all others). Grid boxes without valid data are filled with the "missing" value -31999 for 2-byte integer fields and 0 for 1-byte integer fields.

The code	appears i	in file reac	13B4XRT	$\vec{c}$ .

# Appendix 16.2 \*Read the Header Record, FORTRAN Example\*

The header may be read with most text editor tools, although the size (2880 bytes) may be longer than some tools will support. Alternatively, the header record may be output under program control, as demonstrated in this FORTRAN example. The header is written in a "PARAMETER=VALUE" format, where PARAMETER is a string without embedded blanks that gives the parameter name, VALUE is a string that gives the value of the parameter, and blanks separate each "PARAMETER=VALUE" set. To prevent ambiguity, no spaces or "=" are permitted as characters in either PARAMETER or VALUE.

The	code	e app	ears i	n file <i>r</i>	read_h	eadei	r.f.	
								٠.

## Appendix 16.3 \*Read a File of Data In a Single Read, FORTRAN Example\*

A file of data may be read with many standard data-display tools. The 2880-byte header is designed to be exactly the size of one row of data, so the header may be bypassed by skipping 2880 bytes or 1440 2-byte integer data points or one row. Alternatively, the data may be output under program control using single block reads as demonstrated in this FORTRAN example.

Once past the header, there are always a precipitation field, a random error field, and 1-5 auxiliary fields. As documented in "Data File Layout", the grids are either 1440x720 (3B40RT) or 1440x480 (3B41RT, 3B42RT) and the data are either scaled 2-byte integer (precipitation, random error, and uncalibrated precipitation) or 1-byte integer (all others). Grid boxes without valid data are filled with the "missing" value -31999 for 2-byte integer fields and 0 for 1-byte integer fields.

The code appears in file <i>read_</i>	rt_	file	f.		

# Appendix 16.4 \*Read a File of Data, IDL Example\*

A file of data may be read with many standard data-display tools as demonstrated in the following IDL example. The 2880-byte header is designed to be exactly the size of one row of data, so the header may be bypassed by skipping 2880 bytes or 1440 2-byte integer data points or one row. Alternatively, the data may be output under program control as demonstrated in this IDL example. Once past the header, there are always a precipitation field, a random error field, and 1-5 auxiliary fields. As documented in "Data File Layout", the grids are either 1440x720 (3B40RT) or 1440x480 (3B41RT, 3B42RT) and the data are either scaled 2-byte integer (precipitation, random error, and uncalibrated precipitation) or 1-byte integer (all others). Grid boxes without valid data are filled with the "missing" value -31999 for 2-byte integer fields and 0 for 1-byte integer fields.

The code appears in file read_rt_file.pro.	

# Appendix 16.5 \*Read a File of Data Line-at-a-Time, FORTRAN Example\*

A file of data may be read with many standard data-display tools. The 2880-byte header is designed to be exactly the size of one row of data, so the header may be bypassed by skipping 2880 bytes or 1440 2-byte integer data points or one row. Alternatively, the data may be output under program control using line-at-a-time reads as demonstrated in this FORTRAN example. Once past the header, there are always a precipitation field, a random error field, and 1-5 auxiliary fields. As documented in "Data File Layout", the grids are either 1440x720 (3B40RT) or 1440x480 (3B41RT, 3B42RT) and the data are either scaled 2-byte integer (precipitation, random error, and uncalibrated precipitation) or 1-byte integer (all others). Grid boxes without valid data are filled with the "missing" value -31999 for 2-byte integer fields and 0 for 1-byte integer fields.

The code appears in file <i>read_rt_lines.f</i> .	

## Appendix 16.6 \*Read a File of Data, R Code\*

R code is	popu	ılar with	statisticians	and	other users,	so sample l	R code	read progra	ms have	been
provided	by	Barry	Rowlingson	of	Lancaster	University	(UK).	Please	contact	him
(b.rowling	gson(	alancast	er.ac.uk) if y	ou h	ave any que	stions regard	ling the	R code dist	tribution.	

The R code distribution is	is available at	https://github.	.com/barryrov	vlingson/trmm .